nature cancer

ARTICLES

https://doi.org/10.1038/s43018-021-00275-9

Check for updates

OPEN

Functional antibody and T cell immunity following SARS-CoV-2 infection, including by variants of concern, in patients with cancer: the CAPTURE study

Annika Fendler[1,45], Lewis Au[1,2,45], Scott T. C. Shepherd[1,2,45], Fiona Byrne[1], Maddalena Cerrone[3,4], Laura Amanda Boos[2], Karolina Rzeniewicz[1], William Gordon[1], Benjamin Shum[1,2], Camille L. Gerard[1], Barry Ward[1], Wenyi Xie[1], Andreas M. Schmitt[2], Nalinie Joharatnam-Hogan[2], Georgina H. Cornish[5], Martin Pule[6,7], Leila Mekkaoui[7], Kevin W. Ng[5], Eleanor Carlyle[2], Kim Edmonds[2], Lyra Del Rosario[2], Sarah Sarker[2], Karla Lingard[2], Mary Mangwende[2], Lucy Holt[2], Hamid Ahmod[2], Richard Stone[8], Camila Gomes[8], Helen R. Flynn[9], Ana Agua-Doce[10], Philip Hobson[10], Simon Caidan[11], Michael Howell[12], Mary Wu[12], Robert Goldstone[13], Margaret Crawford[13], Laura Cubitt[13], Harshil Patel[14], Mike Gavrielides[15], Emma Nye[8], Ambrosius P. Snijders[9], James I. MacRae[16], Jerome Nicod[13], Firza Gronthoud[17], Robyn L. Shea[17,18], Christina Messiou[19], David Cunningham[20], Ian Chau[20], Naureen Starling[20], Nicholas Turner[21,22], Liam Welsh[23], Nicholas van As[24], Robin L. Jones[25], Joanne Droney[26], Susana Banerjee[27], Kate C. Tatham[28,29], Shaman Jhanji[28], Mary O'Brien[30], Olivia Curtis[30], Kevin Harrington[31,32], Shreerang Bhide[31,32], Jessica Bazin[33], Anna Robinson[33], Clemency Stephenson[33], Tim Slattery[2], Yasir Khan[2], Zayd Tippu[2], Isla Leslie[2], Spyridon Gennatas[34,35], Alicia Okines[21,34], Alison Reid[36], Kate Young[2], Andrew J. S. Furness[2], Lisa Pickering[2], Sonia Gandhi[37,38], Steve Gamblin[39], Charles Swanton[40,41], The Crick COVID-19 Consortium*, Emma Nicholson[33], Sacheen Kumar[20], Nadia Yousaf[30,34], Katalin A. Wilkinson[3,42], Anthony Swerdlow[43], Ruth Harvey[44], George Kassiotis[5], James Larkin[2], Robert J. Wilkinson[3,4,42], Samra Turajlic[1,2] ✉ and The CAPTURE consortium*

Patients with cancer have higher COVID-19 morbidity and mortality. Here we present the prospective CAPTURE study, integrating longitudinal immune profiling with clinical annotation. Of 357 patients with cancer, 118 were SARS-CoV-2 positive, 94 were symptomatic and 2 died of COVID-19. In this cohort, 83% patients had S1-reactive antibodies and 82% had neutralizing antibodies against wild type SARS-CoV-2, whereas neutralizing antibody titers against the Alpha, Beta and Delta variants were substantially reduced. S1-reactive antibody levels decreased in 13% of patients, whereas neutralizing antibody titers remained stable for up to 329 days. Patients also had detectable SARS-CoV-2-specific T cells and CD4$^+$ responses correlating with S1-reactive antibody levels, although patients with hematological malignancies had impaired immune responses that were disease and treatment specific, but presented compensatory cellular responses, further supported by clinical recovery in all but one patient. Overall, these findings advance the understanding of the nature and duration of the immune response to SARS-CoV-2 in patients with cancer.

Patients with cancer are at increased risk of severe outcomes from coronavirus disease 2019 (COVID-19)[1,2], with risk factors including general features (such as increased age, male sex, obesity and comorbidities) as well as cancer-specific features (such as hematological and thoracic malignancies, progressive cancer and poor performance status)[3–8]. The precise effects of anticancer treatments on the course and outcome of SARS-CoV-2 infection are yet to be fully understood, with different reports yielding conflicting results[5,7,9,10]. Understanding the immune response to SARS-CoV-2 in this heterogeneous population, spanning multiple malignancy types and numerous treatment regimens, is crucial for optimal clinical management of those patients during the ongoing pandemic.

A full list of affiliations appears at the end of the paper.

Previous studies established the features of the acute immune response to SARS-CoV-2 in patients with cancer: (1) patients with solid tumors show high seroconversion rates; (2) patients with hematological cancer show impaired humoral immunity, especially those on anti-CD20 therapy; and (3) higher $CD8^+$ T cell counts in patients with hematological malignancies are associated with improved survival[11–13]. In contrast to the studies above, our cohort consisted mainly of convalescent patients with a range of COVID-19 presentations, from asymptomatic to severe disease. Furthermore, we present an integrated analysis of functional immune response, including SARS-CoV-2-specific T cells and neutralizing antibodies, and cross-protection against emerging variants of concern (VOCs).

CAPTURE (COVID-19 antiviral response in a pan-tumor immune monitoring study) is a prospective, longitudinal cohort study initiated in response to the global SARS-CoV-2 pandemic and its impact on patients with cancer[14]. The study aims were to evaluate the impact of cancer and cancer therapies on the immune response to SARS-CoV-2 infection and COVID-19 vaccination. Here, we report findings from the SARS-CoV-2 infection cohort of the CAPTURE study.

Results

Patient demographics and baseline characteristics. Between 4 May 2020 and 31 March 2021 (database lock), 357 unvaccinated patients with cancer were evaluable with a median followup of 154 d (interquartile range (IQR), 63–273 d). Their median age was 59 years, 54% were male, 89% had a diagnosis of solid malignancy, and the majority (64%) had advanced disease (Table 1). Overall, 118 patients (33%; 97 with solid cancers and 21 with hematological malignancies) were classified as SARS-CoV-2 positive according to our case definition (positive SARS-CoV-2 RT–PCR (PCR with reverse transcription) and/or ELISA (enzyme-linked immunosorbent assay) for S1-reactive antibodies at or before study enrollment) and were included in the analysis (Fig. 1a,b; Methods). Distinct from a population screening program, the intentional recruitment of patients with suspected or confirmed SARS-CoV-2 infection within the study framework (Methods) led to a higher proportion of infected patients than the community prevalence in the United Kingdom within the same time frame. The most common comorbidities were hypertension (27%), obesity (21%) and diabetes mellitus (11%); no significant baseline differences were observed between patients with solid malignancies and those with hematological malignancies (Table 2 and Supplementary Table 1). Overall, 88% of patients received systemic anti-cancer therapy (SACT) in the 12 weeks before infection (51% chemotherapy, 21% targeted therapy, 12% immune-checkpoint inhibitors (CPIs) and 5% anti-CD20), and 10% had radiotherapy and 13% underwent surgery in the 12 weeks before infection. Response to the most recent anti-cancer intervention is shown in Table 2.

Table 1 | CAPTURE cohort overview

	Cohort	SARS-CoV-2 infection	No SARS-CoV-2 infection
Cohort characteristics	$n=357$	$n=118$	$n=239$
Age, years (median, range)	59 (18–87)	60 (18–87)	60 (26–82)
Male, *n* (%)	192 (54)	64 (54)	128 (54)
Cancer diagnosis, *n* (%)			
Skin	79 (22)	10 (8)	69 (29)
Gastrointestinal	71 (20)	30 (25)	39 (16)
Urology	62 (17)	15 (12)	48 (20)
Lung	41 (11)	8 (7)	33 (14)
Hematological	39 (11)	21 (17)	17 (7)
Breast	31 (9)	16 (13)	16 (7)
Gynecological	22 (6)	9 (7)	13 (5)
Sarcoma	12 (3)	4 (3)	8 (3)
Head and neck	6 (2)	5 (4)	1 (0)
Other	4 (1)	4 (3)	0 (0)
Cancer stage, *n* (%)			
Stage I–II	20 (6)	7 (6)	13 (5)
Stage III	72 (20)	22 (18)	50 (22)
Stage IV	229 (64)	70 (58)	159 (67)
Hematological	39 (11)	21 (17)	17 (7)
Days of follow-up, median (IQR)	154 (63–273)	110 (58–274)	164 (63–274)

Viral shedding and lineage. SARS-CoV-2 infection was confirmed by SARS-CoV-2 RT–PCR in 95 of 118 patients (81%). Repeat testing was not mandated by study protocol, but 40% of the patients (47 of 118) had longitudinal swabs during the course of routine clinical care. Within this group, the estimated median duration of viral shedding (Methods) was 12 d (range, 6–80 d) (Fig. 1c and Table 3), with evidence of prolonged shedding in patients with hematological malignancies (median 21 d, versus 12 d in patients with solid cancers) (Extended Data Fig. 1a). Duration of viral shedding did not correlate with COVID-19 severity ($r=0.04$, $P=0.7$). We performed viral sequencing in 52 RT–PCR-positive samples with $Ct<32$ (Methods), of which 44 of 52 passed sequencing quality control. The Alpha VOC accounted for the majority of infections in our cohort between December 2020 and March 2021, consistent with community prevalence in the United Kingdom at that time (Extended Data Fig. 1b).

Clinical correlates of COVID-19 severity in patients with cancer. Overall, 94 patients (80%) were symptomatic, of whom 52 (44%) had mild illness, 36 (31%) had moderate illness and 6 (5%) had severe illness (as per the World Health Organization (WHO)

Fig. 1 | SARS-CoV-2 infection status, viral shedding and COVID-19 symptoms of recruited patients. a, Patients with cancer irrespective of cancer type, stage or treatment were recruited. Follow-up schedules for patients with cancer were bespoke to their COVID-19 status and account for their clinical schedules (inpatients, every 2–14 d; outpatients, every clinical visit maximum every 3–6 weeks in year one and every 6 months in year two and at the start of every or every second cycle of treatment). Clinical data, ONP swabs and blood were collected at each study visit. Viral antigen testing (RT–PCR on swabs), antibody (ELISA and flow cytometric assay), T cell response and IFN-γ activation assays were performed. **b**, Distribution of SARS-CoV-2 infection and S1-reactive antibody status and COVID-19 severity in patients with cancer. In total, 357 patients with cancer were recruited between 4 May 2020 and 31 March 2021. SARS-CoV-2 infection status by RT–PCR and S1-reactive antibodies were analyzed at recruitment and in serial samples. RT–PCR results before recruitment were extracted from electronic patient records. The COVID-19 case definition included all patients with either RT–PCR-confirmed SARS-CoV-2 infection or S1-reactive antibodies. **c**, Viral shedding in 43 patients with serial positive swabs. Solid bars indicate time to the last positive test and dotted lines denote the time from the last positive test to the first negative test. **d**, Distribution of symptoms in 118 patients with COVID-19. Bar graph denotes the number of patients. Each row in the lower graph denotes one patient. ONP, oronasopharyngeal; WGS, whole-genome sequencing; RTx, radiotherapy; HSCT, human stem cell transplant; GI, gastrointestinal.

severity scale[15]; Table 3); 24 patients (20%) were asymptomatic (WHO score 1). Among all patients ($n=118$), fever (47%), cough (42%), dyspnea (31%) and gastrointestinal symptoms (12%) were the most common presenting symptoms (Fig. 1d), with a median of 2 symptoms reported (range, 0–7). In patients with a clear date of symptom resolution ($n=77$), median duration of symptoms was

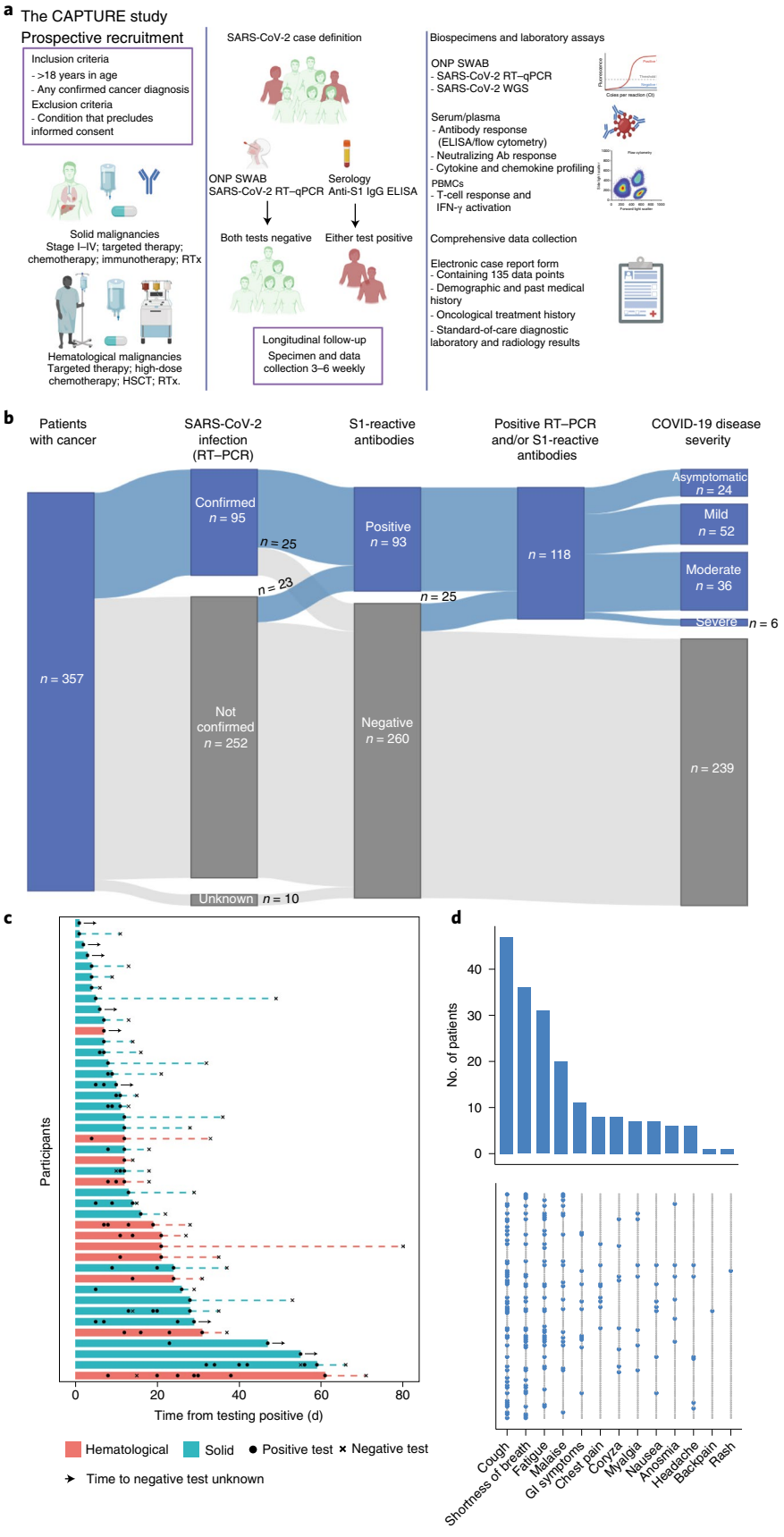

Table 2 | Oncological and medical history of patients positive for SARS-CoV-2

N = 118	
Past medical history	
HTN	31 (27)
PVD/IHD/CVD	9 (8)
Diabetes mellitus	14 (11)
Obesity, BMI > 30, *n* (%)	25 (21)
Inflammatory/autoimmune	7 (6)
Smoking status	
Current smoker	36 (31)
Ex-smoker	51 (43)
Never smoked	12 (10)
Unknown	19 (16)
Oncological history	
Solid tumors, *n* = 97	
Disease status (in respect to last treatment)	
SACT, palliative, *n* = 74	
CR/PR	27 (28)
SD	24 (24)
PD	23 (24)
SACT, neoadjuvant or radical CRT	8 (8)
Surgery ± adjuvant SACT	15 (15)
Treatment within 12 weeks	
Systemic therapy	
Chemotherapy	43 (44)
Small molecule inhibitor	15 (15)
Anti-PD-(L)1 ± anti-CTLA-4	14 (14)
Endocrine therapy	7 (6)
No treatment	5 (4)
Local therapy	
Surgery	15 (13)
Radiotherapy	11 (10)
Hematological malignancies, *n* = 21	
Diagnosis	
Acute leukemia	11 (52)
Lymphoma	6 (29)
Myeloma	4 (19)
Disease status	
MRD/CR	5 (24)
Partial remission	7 (33)
SD	3 (14)
PD/relapse/untreated acute presentation	7 (33)
Treatment within 12 weeks	
Chemotherapy	17 (81)
Targeted therapy	10 (48)
Anti-CD20 therapy	6 (29)
CAR-T	1 (5)
Hematological stem cell transplant	
Auto/allograft pre-COVID-19	6 (29)
Auto/allograft post-COVID-19	2 (9)

BMI, body mass index; CAR-T, chimeric antigen receptor T cell; CD20, B-lymphocyte antigen; CR, complete response; CRT, chemoradiotherapy; CTLA-4, cytotoxic T-lymphocyte-associated protein 4; CVD, cardiovascular disease; HTN, hypertension; IHD, ischemic heart disease; MRD, minimal residual disease; PD progressive disease; PR, partial response; PVD, peripheral vascular disease;SD, stable disease.

Table 3 | Clinical characteristics of COVID-19 illness

COVID-19 characteristics	*n* (%)
Viral shedding status	
PCR-positive, *n* (%)	95 (81)
Duration of PCR positivity, days median (range)	12 (6–80)
WHO Severity Score	
1, Asymptomatic	24 (20)
2–3, Mild	52 (44)
4–5, Moderate	36 (31)
>5, Severe	6 (5)
Admission to hospital	
Not hospitalized	54 (49)
Admitted with COVID-19-like illness	33 (29)
COVID-19 illness during hospitalization	30 (25)
Duration of admission, days median (range)	9 (1–120)
Complications of COVID-19	
Required supplemental oxygen	27 (23)
Pneumonia	29 (25)
Venous/arterial thromboembolism	9 (8)
Admission to intensive therapy unit	7 (6)
Need for mechanical ventilation/NIV	4 (3)
COVID-19-directed therapy	
Corticosteroids	13 (11)
Anti-IL-6 monoclonal antibody	3 (3)
Laboratory investigations, median (IQR)	
Hematology	
Hb, g l^{-1}	110 (93–128)
WBC, $\times 10^6$ l^{-1}	5.7 (3.4–8.0)
N0, $\times 10^6$ l^{-1}	3.8 (2.1– 5.5)
Plt, $\times 10^6$ l^{-1}	213 (130–299)
Biochemistry	
Creatinine, μmol l^{-1}	60 (53–71)
CRP, mg l^{-1}	59 (23–134)
Clinical outcomes and impact	
Survival	
Deceased, *n* (%)	13 (10)
Death within 30 d of PCR positivity	4 (3)
Primary cause death:	
Progressive cancer	11 (9)
Complications of COVID-19	2 (2)

CRP, C-reactive protein; Hb, hemoglobin; N0, neutrophil; NIV, noninvasive ventilation; Plt, platelet; WBC, white blood cell.

18 d (IQR, 11–30 d). Three patients met the criteria of long COVID (symptomatic >90 d since presentation of disease (POD)), all following severe COVID-19 requiring care in an intensive therapy unit.

Thirty-three patients (28%) were hospitalized due to COVID-19, with a median duration of inpatient stay of 9 d (range, 1–120 d); twenty-seven (23%) required supplemental oxygen, and seven (6%) were admitted to an intensive care unit, with one (1%) requiring mechanical ventilation and inotropic support (Table 3). Thirteen patients (11%) were treated with corticosteroids (>10 mg prednisolone equivalent), and three patients (3%) received treatment with a monoclonal antibody to IL-6. Nine patients (8%) had a thromboembolic

complication. At database lock, eleven SARS-CoV-2-positive patients (9%) died of progressive cancer, and two patients (2%) died due to recognized complications of COVID-19 (Table 3).

The risk of moderate and severe COVID-19 was associated with hematological malignancies, whereas the risk of severe COVID-19 in solid malignancies was associated with progressive disease under SACT (Supplementary Table 2), in line with previous reports[7,8,12]. We found no association between COVID-19 severity, cancer stage, performance status, sex, age, obesity, smoking status or comorbidities across the whole cohort, in contrast to reports from cancer registries, which largely reflected patients who were hospitalized with COVID-19 (refs. [4,6–8,16]) and the general population[17]. Furthermore, our relatively small cohort size probably also contributed to the lack of association with these factors.

Cytokine profiles and disease severity during infection. Owing to our study design (Fig. 1a), recruitment was biased toward patients within the convalescent stage of SARS-CoV-2 infection. Only 27 patients (23%) were recruited while still SARS-CoV-2 RT–PCR positive, and 3 (3%) became SARS-CoV-2 RT–PCR positive after recruitment to CAPTURE. Cytokine/chemokine profiling indicated only a non-significant increase in cytokine concentrations in SARS-CoV-2-infected patients (eight with solid tumors and six with hematological malignancies) relative to that in uninfected patients with cancer ($n=5$) (Extended Data Figure 1c,d; Methods). Notably, the concentrations of interferon (IFN)-γ, interleukin (IL)-18, IL-6, IL-8, IL-9, IP-10 and macrophage inflammatory protein (MIP)1-β correlated with severe disease (Extended Data Fig. 1e,f). The concentration of IFN-γ and IL-18 in serum was significantly higher in patients with hematological malignancies than in those with solid cancer during acute infection (Extended Data Fig. 1g).

S1-reactive SARS-CoV-2 antibody response in patients with cancer. We evaluated total S1-reactive antibody titers by ELISA at multiple time points during follow-up (with two median samples per patient (range, 1–11)) in 112 patients; 6 patients (5%) were excluded, as blood samples were unavailable or were obtained after COVID-19 vaccination. In total, 93 of 112 patients (83%) had detectable antibodies. S1 antibodies were detectable in 74 of 89 symptomatic patients (83%) and in 19 of 23 asymptomatic patients (83%). S1-reactive antibody titers were associated with COVID-19 severity ($P=0.074$) (Fig. 2a).

Nineteen patients (17%), with median follow up of 22 d (range, 0–301 d), had no evidence of S1-reactive antibodies following a positive SARS-CoV-2 RT–PCR. Lack of seroconversion was significantly associated with hematological malignancies: 9 of 20 patients (45%) with hematological malignancies versus 10 of 92 patients (11%) with solid malignancies did not seroconvert (chi-squared test, $P=0.0002$). In addition, S1-reactive antibody titers were significantly lower in patients with hematological malignancies than in those with solid malignancies (Fig. 2b). Two patients with long COVID had no evidence of seroconversion at any point during follow-up (followed for 222 d and 235 d after disease onset, respectively).

We conducted a sensitive flow cytometric assay on serum from a subset of patients with S1-reactive antibodies($n=40$; Extended Data Figs. 2a and 3) and detected S-specific IgG in 38 of 40 patients (95%) (Extended Data Fig. 2b) and IgM in 23 of 40 patients (58%) (Extended Data Fig. 2c). IgG and IgM levels significantly correlated with S1-reactive antibody titers ($P<0.0001$) (Extended Data Fig. 2e,f). S-reactive IgA was detected in only four convalescent patients (10%) (Extended Data Fig. 2d), consistent with its role in the early response to SARS-CoV-2 infection[17].

Finally, we evaluated matched pre-pandemic serum samples from 47 patients: 10 with and 37 without evidence of S1-reactive antibodies in post-pandemic serum. We found no evidence of S1-reactive antibodies in the pre-pandemic serum of any patient (Extended Data Fig. 2g). However, S-reactive IgG or IgM was detected in serum in 18 patients without confirmed SARS-CoV-2 infection, indicating cross-reactivity to seasonal human coronaviruses, with more frequent cross-recognition of the S domain than of the more conserved S1 domain, as reported in individuals without cancer[18].

NAbs against SARS-CoV-2 VOCs in patients with cancer. We assessed neutralizing antibodies (NAbs) in all patients using a high-throughput a live-virus neutralization assay (Methods), against wild-type (WT) SARS-CoV-2 and the Alpha (B.1.1.7), Beta (B.1.351) and Delta (B.1.617.2) VOCs, and results are presented as titers (the reciprocal of serum required to inhibit 50% of viral replication (IC_{50})). NAb titers below 40 were considered undetectable (Methods).

We detected NAbs against WT SARS-CoV-2 in 88 of 93 patients (95%) with S1-reactive antibodies (in 77 of 82 (94%) with solid tumors and in 11 of 11 (100%) with hematological malignancy). NAbs were detected in 4 of 19 RT-PCR-positive patients without S1-reactive antibodies (21%) (in 2 of 10 (20%) with solid cancer and in 2 of 9 (22%) with hematological malignancy). NAb titers were significantly associated with COVID-19 severity (Fig. 2c).

In a binary logistic regression model including all patients with cancer ($n=112$), presence of hematological malignancy, but not comorbidities, age, sex or COVID-19 severity, was associated with undetectable NAbs (Fig. 2e). Accordingly, median NAb titers against WT SARS-CoV-2 were lower in patients with hematological malignancies than in those with solid cancer (Fig. 2d).

In patients with solid cancer ($n=92$), cancer type, stage, progressive disease and cancer therapy (Fig. 2f,g) were not associated

Fig. 2 | S1-reactive and antibody response in patients with cancer. a, S1-reactive antibody titers (AbT) by COVID-19 severity ($n=112$ patients). Significance was tested by Kruskal–Wallis test, $P=0.074$. **b**, S1-reactive antibody titers by cancer type (solid, $n=92$; hematological, $n=20$). Significance was tested by two-sided Wilcoxon–Mann–Whitney *U*-test, $P=0.011$. **c**, NAb titers (NAbT) by COVID-19 severity ($n=112$ patients). Significance was tested by Kruskal–Wallis test, $P=0.0027$. **d**, NAb titers by cancer type (solid, $n=92$; hematological, $n=20$). Significance was tested by two-sided Wilcoxon–Mann–Whitney *U*-test, $P=0.052$. Boxes indicate 25th and 75th percentiles, line indicates median and whiskers indicate 1.5 × IQR. Dots represent individual samples. Dotted lines and gray boxes denote the limit of detection. **e**, Multivariate binary logistic regression evaluating association with lack of NAb in patients with cancer ($n=112$). Wald *z*-statistic was used two calculate two-sided *P* values. *$P=0.038$. **f**, Multivariate binary logistic regression evaluating the association of lack of NAb in patients with solid cancer ($n=92$). **g**, Multivariate binary logistic regression evaluating the association of lack of NAb in patients with solid cancer ($n=92$). Dot denotes odds ratio (blue, positive odds ratio; red, negative odds ratio); whiskers indicate 1.5 × IQR. **h**, NAb titers against WT, Alpha, Beta and Delta VOCs in patients ($n=112$) infected with WT SARS-CoV-2 or Alpha VOC. Violin plots denote density of data points. Point range denotes median and 25th and 75th percentiles. Dots represent individual samples. Significance was tested by Kruskal–Wallis test, $P=3.5\times10^{-7}$, two-sided Wilcoxon–Mann–Whitney *U*-test with Bonferroni correction (post hoc test) was used for pairwise comparisons. *P* values are denoted in the graph. **i**,**j**, S1-reactive antibody titers (**i**) and NAb titers (**j**) after onset of disease ($n=97$ patients). Blue line denotes loess regression line with 95% confidence bands in gray. Black dots denote patients with one sample and colored dots denote patients with serial samples ($n=51$ patients). Samples from individual patients are connected. Dotted lines and gray areas at the bottom indicate limit of detection.

with undetectable NAbs. Due to limited sample size, patients with hematological malignancies ($n=20$) could not be evaluated by a multivariate model.

In patients infected with WT SARS-CoV-2 ($n=85$) or the Alpha VOC ($n=27$), the proportion of patients with detectable NAbs against VOCs was significantly lower than those with detectable

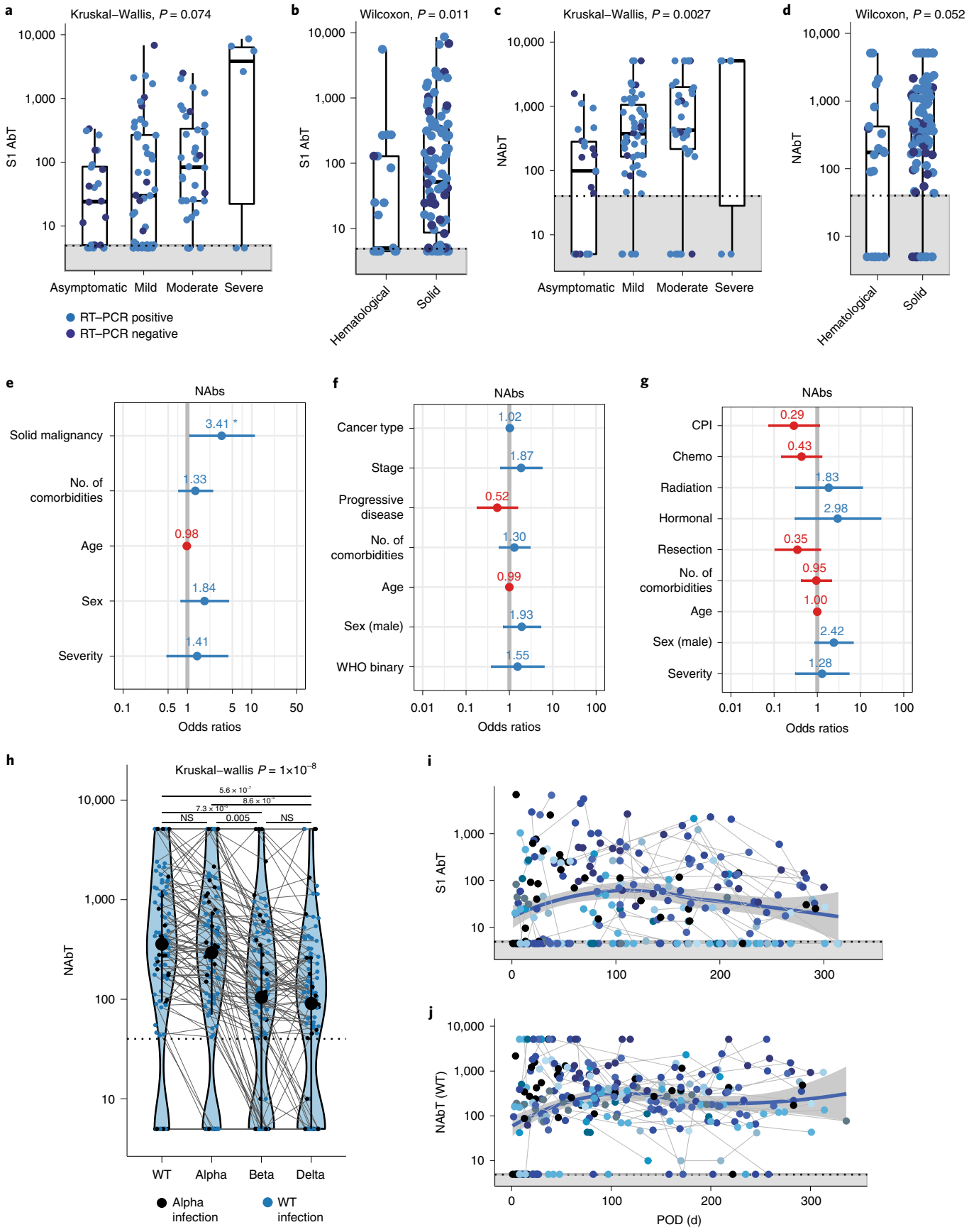

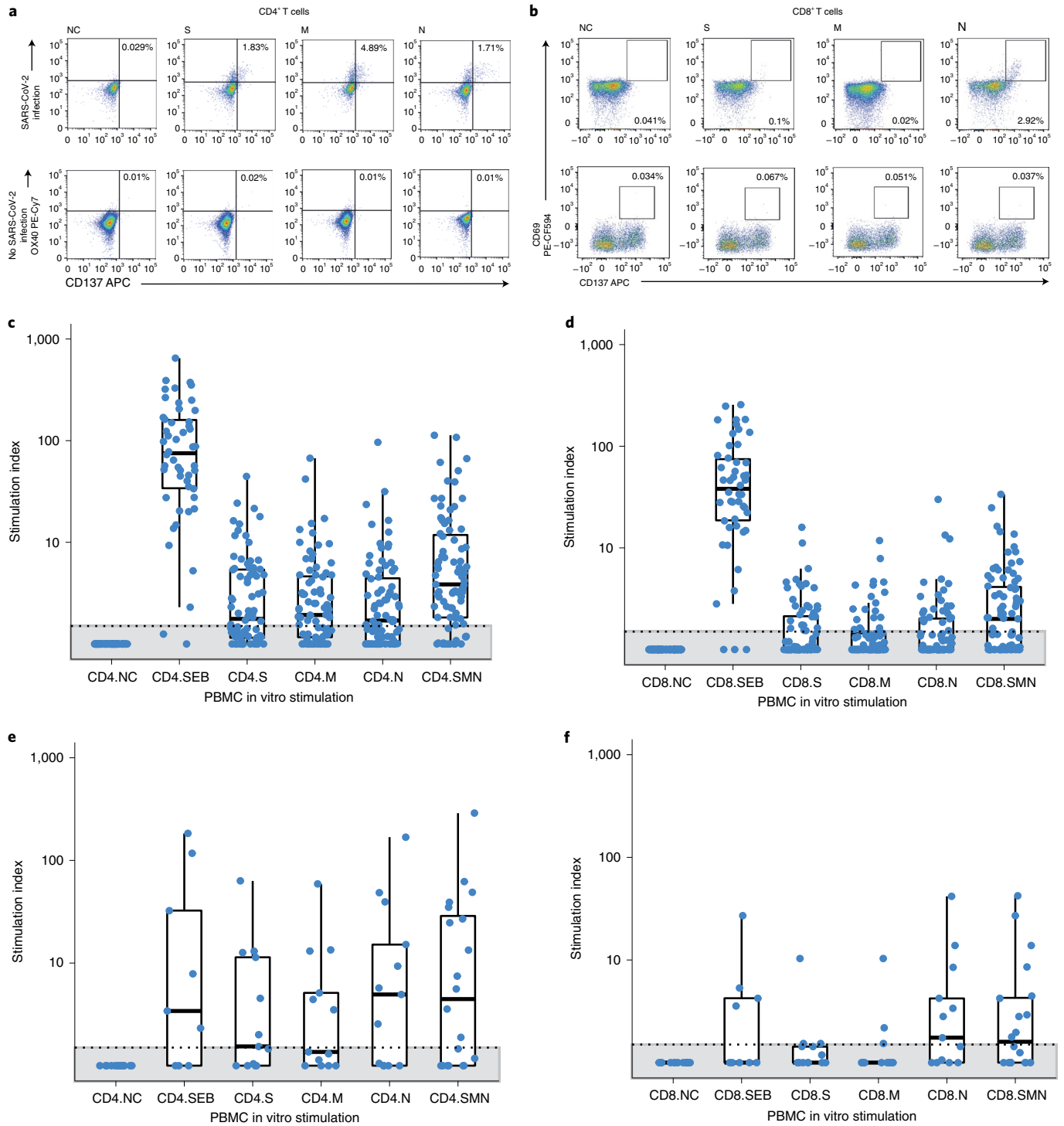

Fig. 3 | T cell response in patients with cancer. a,**b**, Representative plots of CD4$^+$CD137$^+$OX40$^+$ (CD4$^+$) and CD8$^+$CD137$^+$CD69$^+$ (CD8$^+$) T cells in a patient with confirmed COVID-19 and a cancer patient without COVID-19 after in vitro stimulation with S, M and N peptide pools, positive control Staphylococcal enterotoxin B (SEB) or negative control (NC). **c**,**d**, Frequency of SARS-CoV-2-specific CD4$^+$ (**c**) and CD8$^+$ (**d**) T cells in patients with solid malignancies ($n=83$). **e**,**f**, Frequency of SARS-CoV-2-specific CD4$^+$ (**e**) and CD8$^+$ (**f**) T cells in patients with hematological malignancies ($n=21$). The stimulation index was calculated by dividing the percentage of positive cells in the stimulated sample by the percentage of positive cells in NC. To obtain the total number of SsT cells, the sum of cells activated by S, M and N was calculated (SMN). Boxes indicate the 25th and 75th percentiles, the line indicates the median and whiskers indicate 1.5 × IQR. Dots represent individual samples. Dotted lines and gray boxes denote the limit of detection.

NAbs against WT SARS-CoV-2 (WT, 92 of 112 (82%); Alpha, 89 of 112 (79%); Beta, 77 of 112 (69%); Delta, 73 of 112 (65%); chi-squared test, $P=0.009$), and the median NAb titers against Beta and Delta were significantly lower than those against WT and Alpha (Fig. 2h). The proportion of patients with detectable NAbs against all variants was significantly lower in patients with hematological malignancies than in those with solid cancer (WT, 86% versus 65%, chi-squared test, $P=0.03$; Alpha, 84% versus 60%, chi-squared test,

$P=0.02$; Beta, 74% versus 45%, chi-squared test, $P=0.01$; Delta, 71% versus 40%, chi-squared test, $P=0.009$).

There was a significant correlation between the levels of S1-reactive antibody and NAb titers against WT SARS-CoV-2 and all VOCs ($P<0.0001$) (Extended Data Fig. 2h). However, the proportion of patients with detectable S1-reactive antibodies without detectable NAbs was greater for the VOCs than for WT SARS-CoV-2 (WT, 5 of 93 (5%); Alpha, 7 of 93 (8%); Beta, 17 of 93 (18%); Delta, 20 of 93 (22%); chi-squared test, $P=0.002$).

SARS-CoV-2 antibody response lasts up to 11 months. Next, we assessed antibody kinetics in 59 of 97 patients (61%) ($n=45$ with solid cancer and $n=14$ with hematological malignancy) with detectable S1-reactive antibodies in whom the time of disease onset was known (median of two time points per patient (range, 2–10); median length of follow-up, 181 d (range, 8–336 d)). Five patients were followed for more than 300 d. Follow-up samples collected after COVID-19 vaccination were excluded.

Thirty-three (56%) had S1-reactive antibodies at the time of enrollment (median of 69 d post onset of disease (POD) (range, 3–217 d); Fig. 2i), and a further five (8%) seroconverted within 13–117 d POD. S1-reactive antibody titers showed a weak declining trend, and 14 of 59 patients (24%) became seronegative 24–313 d POD (including 2 of 5 patients with delayed seroconversion). Most of those (12 of 14) had solid cancer and no clinical features that could conceivably account for the short-lived antibody response. Two patients with hematological malignancy who did not sero-convert included one with a diagnosis of T cell acute lymphoblastic leukemia who had a stem cell transplant complicated by chronic graft-versus-host disease after recovering from COVID-19, and and one patient with plasmablastic lymphoma treated with anti-CD20 prior to SARS-CoV-2 infection.

NAbs against all variants were detected as early as day 1 in the 59 patients (Fig. 2j and Extended Data Fig. 4a–c) and as late as day 217 POD, and NAb titers remained stable overall up to 336 d. In the group of patients who sero-reverted (S1 antibodies became undetectable during follow-up), NAbs against WT SARS-CoV-2 remained detectable in 10 of 14 (71%) (Alpha, 9 of 14 (64%); Beta, 2 of 14 (14%); Delta, 2 of 14 (14%)).

SARS-CoV-2-specific T cells are detected in patients with cancer. Peripheral blood mononuclear cell (PBMC)-stimulation assays (Methods) were performed in 110 of 112 patients who were SARS-CoV positive (81 with solid cancer and 19 with hematological malignancy; Extended Data Fig. 3b); 12 of 112 samples were excluded (for lack of PBMC collection, low viability, or no detection of $CD3^+$ cells in activation-induced marker). SARS-CoV-2-specific $CD4^+$ and $CD8^+$ T cells (SsT cells; identified by activation-induced markers OX40, CD137 and CD69)[19] were quantified at the first time point after seroconversion, at a median of 59 d POD (range, 1–292 d) (Fig. 3a,b). We detected SARS-CoV-2-specific $CD4^+$ T cells in 77 of 100 patients (77%) and $CD8^+$ T cells in 49 of 100 patients (49%) (Fig. 3c–f). $CD8^+$ T cells levels were consistently lower than $CD4^+$ T cell levels (Extended Data Fig. 5a), a result also noted in participants without cancer[20–22], possibly reflecting our use of 15-mer peptide pools for stimulation, which could favor detection of CD4 responses over that of CD8 responses.

$CD4^+$ T cells were detected in 81% of patients with solid malignancies and in 58% of patients with hematological malignancies (Fig. 3c,e). $CD8^+$ T cells were detected in similar proportions of patients with solid malignancies and those with hematological malignancies (51% and 42%, respectively) (Fig. 3d,f).

Consistent with functional activation of SsT cells, after in vitro stimulation of PBMCs, we detected increased levels of IFN-γ in culture supernatants, which correlated with the number of SsT cells (Extended Data Fig. 5b). IFN-γ levels did not differ between patients with solid cancers versus those with hematological malignancies (Extended Data Fig. 5c).

Finally, to account for the lack of matched pre-infection samples in our cohort, and given reports of cross-reactive T cell responses to other human coronaviruses in healthy individuals[19,23], we extended the T cell assay to 12 patients with cancer without confirmed SARS-CoV-2 infection. Cross-reactive $CD4^+$ T cells were detected in 7 of 12 participants and $CD8^+$ T cells were detected in 3 of 12 participants, but the overall level SsT cells was significantly lower in uninfected patients than in patients with confirmed SARS-CoV-2 infection ($P<0.05$) (Extended Data Fig. 5d,e).

SsT cell compensation in patients without humoral response. Patients with hematological malignancies had a wide range of S1, NAb and SsT cell responses (Fig. 4a,b,c). Among patients with leukemia, NAbs were detected in 9 of 11 and SsT cells were detected in 5 of 10 evaluable patients (2 had both $CD4^+$ and $CD8^+$ responses; 2 had $CD4^+$ only responses; and 1 had a $CD8^+$ only response). Among patients with myeloma, two of three had NAbs, and two of three had detectable SsT cells ($CD4^+$ and $CD8^+$). Finally, two of six patients with lymphoma had detectable NAbs, whereas SsT cells were detected in five of six (three had both $CD4^+$ and $CD8^+$ responses; one had a $CD4^+$ only response; and one had a $CD8^+$ only response). Overall, SsT cell levels were higher in patients with lymphoma than in those with leukemia (Fig. 4c). Four of five patients with lymphoma given anti-CD20 treatment had no NAb response (Fig. 4d,e). The fifth patient with plasmablastic lymphoma had detectable NAb titers against WT SARS-CoV-2 and the Alpha VOC. In contrast, NAb titers against Beta and Delta and S1-reactive antibody titers were detected at only one time point before the patient sero-reverted at 37 d POD. One additional patient with a diagnosis of acute myeloid leukemia, with a history of allogeneic stem-cell transplant and treatment with anti-CD20, had no NAbs, and SsT cells could not be evaluated. Four of five patients with lymphoma given anti-CD20 treatment had detectable SsT cells, and their levels of SsT cells were not lower than those in patients not treated with anti-CD20 (Fig. 4f). In patients with solid malignancies, the levels of NAbs and SsT cells did not differ significantly by tumor type (Figs. 2f and 4g, respectively).

Fig. 4 | Comparison of antibody and T cell responses in patients with cancer. a, S1-reactive antibody titers in patients with leukemia ($n=11$), myeloma ($n=4$) and lymphoma ($n=6$). **b**, NAb titers in patients with leukemia ($n=10$), myeloma ($n=4$) and lymphoma ($n=6$). **c**, $CD4^+$ and $CD8^+$ cells T cells in patients with leukemia ($n=10$), myeloma ($n=4$) and lymphoma ($n=6$). The stimulation index was calculated by dividing the percentage of $CD4^+CD137^+OX40^+$ ($CD4^+$) and $CD8^+CD137^+CD69^+$ ($CD8^+$) T cells in the stimulated sample by the percentage of positive cells in the NC. Significance was tested by Kruskal–Wallis test, where $P<0.05$ was considered significant. **d**, S1-reactive antibody titers in patients with hematological malignancy receiving anti-CD20 treatment ($n=6$) versus other SACT ($n=15$). **e**, NAb titers in patients with hematological malignancy receiving anti-CD20 treatment ($n=6$) versus other SACT ($n=15$). Significance was tested by two-sided Wilcoxon–Mann–Whitney *U*-test, where $P<0.05$ was considered significant. **f**, Comparison of $CD4^+/CD8^+$ T cells between patients with hematological malignancies on anti-CD20 therapy ($n=5$, administered within 6 months) and not on anti-CD20 therapy ($n=15$). Significance was tested by two-sided Wilcoxon–Mann–Whitney *U*-test, where $P<0.05$ was considered significant. **g**, $CD4^+$ and $CD8^+$ cells T cells in patients with solid malignancies ($n=81$) by cancer subtype. Boxes indicate 25th and 75th percentiles, the line indicates the median and whiskers indicate 1.5 × IQR. Dots represent individual patient samples. Dotted lines and gray boxes denote the limit of detection. Significance was tested by Kruskal–Wallis test, where $P<0.05$ was considered significant.

Overall, we observed a discordance between antibody responses and T cell responses among patients with hematological malignancy. First, a greater proportion of patients with detectable NAb titers had detectable CD4+ T cells than that of patients without detectable NAb titers (among NAb-positive patients, 9 of 13 (69%); among NAb-negative patients, 2 of 6 (33%)), and we observed no correlation

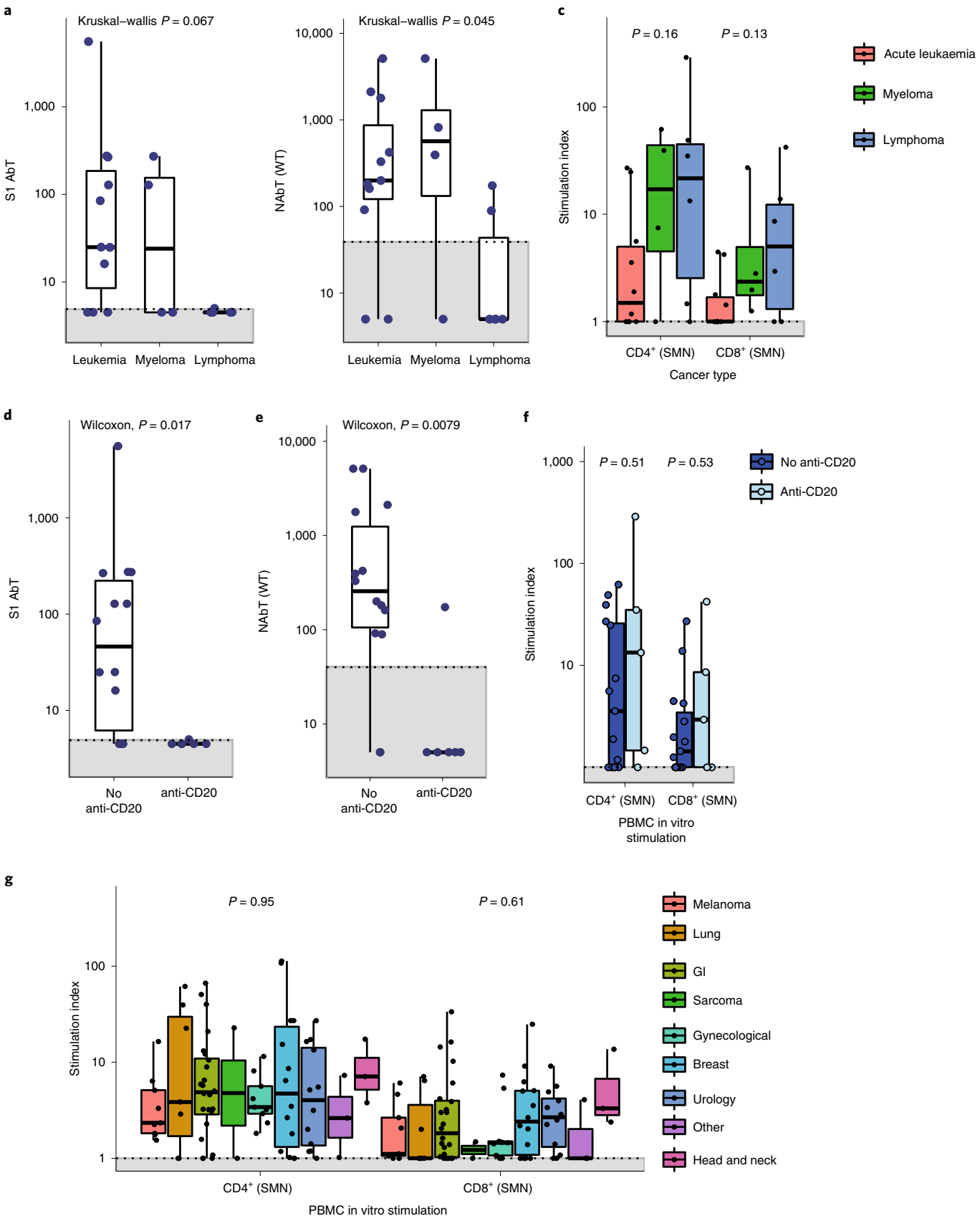

of S-reactive CD4+ T cell levels and NAb titers (Extended Data Fig. 5g). Second, 2 of 6 patients with undetectable NAb titers (33%) still had detectable CD8+ T cells, compared with 7 of 13 patients with detectable NAb titers (54%) (Supplementary Table 3).

Among patients with solid cancer, the proportion of patients with detectable CD4+ T cells or detectable CD8+ T cells was lower for those with undetectable NAb titers (CD4+, 8 of 12 (67%); CD8+, 2 of 12 (17%)) than for those with detectable NAb titers (CD4+, 58 of 69 (84%); CD8+, 39 of 69 (57%)) (Supplementary Table 3). We further observed a significant correlation of S-reactive CD4+ T cell levels and NAb titers against WT SARS-CoV-2 (Extended Data Fig. 5f).

Finally, following stimulation with S and N pools, we observed that patients with hematological malignancy exhibited higher levels of N-reactive CD8+ T cells than S-reactive CD8+ T cells (Fig. 3e,f), whereas similar levels were observed in patients with solid cancer (Fig. 3c,d), indicating that antigens other than spike (S) may contribute to T cell responses in patients with hematological malignancies.

T cell responses are impacted in CPI-treated patients. Next, we evaluated features associated with impaired T cell responses to SARS-CoV-2 in patients with cancer. We found no association between lack of SsT cells and the presence of solid or hematological malignancies, or the number of comorbidities, age, sex or COVID-19 severity (Fig. 5a,b). In patients with solid malignancies, those on CPIs ($n=13$) had significantly reduced levels of SARS-CoV-2-reactive CD4+ T cells (Fig. 5c), and in a binary logistic regression model, lack of SARS-CoV-2-reactive CD4+ (but not CD8+) T cells was associated with CPI therapy within 3 months of SARS-CoV-2 infection (Fig. 5d,e).

Immune responses are lower than in those without cancer. We compared S1-reactive and NAb responses in patients with cancer with those of a control cohort of 21 healthcare workers (HCWs) with SARS-CoV-2 infection who were recruited to CAPTURE. We applied the same case definition as that for patients with cancer (positive SARS-CoV-2 RT–PCR and/or ELISA for S1-reactive antibodies at or prior to study enrolment). Of note, HCWs were not matched to patients with cancer by age, and they represented an overall younger cohort, with a median age of 43 years (IQR, 40–52 years). Seven HCWs (33%) were asymptomatic, and fourteen HCWs (67%) reported mild symptoms, among whom eight (38%) had SARS-CoV-2 infection confirmed by RT-PCR; none were hospitalized. Twenty-one HCWs (100%) had detectable S1-reactive antibodies, and twelve (57%) had detectable NAbs against WT SARS-CoV-2, a lower proportion than that of patients with cancer. S1-reactive antibody titers and NAb titers against WT SARS-CoV-2 were numerically lower in HCWs than in patients with solid malignancies but higher than in patients with hematological malignancies (Extended Data Fig. 6a,b).

We also evaluated SARS-CoV-2-reactive CD4+ and CD8+ T cell levels in the same cohort of HCWs (CD4+ T cells, 16 of 19 (84%); CD8+ T cells, 10 of 19 (53%)). We observed a similar proportion of HCWs with detectable SsT cells as noted for patients with solid cancer. The median SsT cell levels were numerically higher in HCWs than in all patients with cancer (Extended Data Fig. 6c,d).

Discussion

Results from this prospective, longitudinal study of 118 patients with cancer and SARS-CoV-2 infection indicated that most patients with solid tumors developed a functional and probably durable (up to 11 months) humoral immune response to SARS-CoV-2 infection, as well as an anti-SARS-CoV-2-specific T cell response. Patients with hematological malignancies had significantly lower seroconversion rates, and impaired immune responses that were related to both disease and treatment (anti-CD20), although with evidence of compensation, consistent with prior reports[11].

Our findings largely relate to patients with a diagnosis of solid cancer (82% of the cohort), the majority of whom had evidence of seroconversion (89%). Absence of or a delay in seroconversion was observed in 10% of patients with solid tumors, in line with data reported from smaller prospective studies from the United Kingdom (95%, $n=22$)[12] and Italy (88%, $n=28$)[24] and comparable to results in individuals without cancer. We did not observe an obvious impact of solid cancer characteristics on the likelihood of seroconversion. Recent studies of people without cancer demonstrated a clear relationship between neutralizing responses and recovery from infection[25], as well as vaccine efficacy[26,27]. In our cohort, 94% of seroconverted patients with solid tumors also had detectable NAbs (to WT SARS-CoV-2 or the Alpha VOC, consistent with the causative variant). Notably, although we observed a weak decline in S1-reactive antibody titers, NAb titers were stable for at least 7 months and in some cases up to 11 months of follow-up. Discordance was specifically observed in 14 patients with declining S1-reactive antibodies, indicating that these patients had persistent NAbs that were not detected by the S1 ELISA[28].

Longer follow-up was limited by COVID-19 vaccination, which commenced in the United Kingdom in December 2020 (ref. [29]). In individuals without cancer, the reported durability of both SARS-CoV-2-specific IgG and NAbs varies substantially[20,30–33], and direct comparison of our data to those reports is challenging.

We compared antibody and cellular responses in patients with cancer with those of 21 HCWs with SARS-CoV-2 infection. Antibody and cellular responses in patients with hematological malignancies were all lower than those of HCWs. We note that the HCWs all had asymptomatic or mild COVID-19. The association of antibody responses with COVID-19 severity in this cohort and in healthy individuals[34] may explain why we observed numerically higher S1-reactive antibody and NAb titers in patients with solid cancer than in HCWs. We found that SsT cell levels were numerically lower in patients with cancer; cellular responses in healthy individuals show an inverse association with age and disease severity[21]. In summary, the comparison with HCWs confirmed that patients with hematological malignancies had impaired immune responses, while the majority of patients with solid cancer had responses comparable to those of healthy individuals.

In line with data for SARS-CoV-2 convalescent patients without cancer[35], we found that neutralizing activity against the Alpha, Beta, and Delta VOCs was decreased. Of note, we showed that 35% of patients with cancer previously infected with WT or Alpha SARS-CoV-2 lacked NAbs against Delta. In patients who

Fig. 5 | Associations between SARS-CoV-2-specific T cells with patient or cancer-specific features. a,**b**, Multivariate binary logistic regression analysis evaluating associations between SARS-CoV-2-specific CD4+ (**a**) and CD8+ (**b**) T cells with cancer diagnosis (solid versus hematological malignancies), comorbidities, age, sex and COVID-19 disease severity in 100 patients. Wald *z*-statistic was used to calculate two-sided *P* values. **P* = 0.038. **c**,**d**, Multivariate binary logistic regression analysis evaluating associations between SARS-CoV-2-specific CD4+ (**c**) and CD8+ (**d**) T cells with anticancer intervention, age, sex and COVID-19 disease severity in patients with solid cancer ($n=81$). Wald *z*-statistic was used to calculate two-sided *P* values. **P* = 0.045. Dot denotes odds ratio (blue and red dots indicate positive or negative odds ratios, respectively); whiskers indicate 1.5 × IQR. **e**, Comparison of SARS-CoV-2-specific CD4+/CD8+ T cells between patients with solid malignancies taking CPIs ($n=13$, administered within 3 months) and not on CPIs ($n=68$). Boxes indicate the 25th and 75th percentiles, line indicates the median and whiskers indicate 1.5 × IQR. Dots represent individual samples. Significance was tested by two-sided Wilcoxon–Mann–Whitney *U*-test (*P* = 0.038 and *P* = 0.53).

sero-reverted, NAbs against WT SARS-CoV-2 were still detected, while NAb titers against Delta, if present, declined over time. This raises concerns about considering a history of prior infection with one variant as evidence of functional immunity against VOCs. Finally, given that the majority of patients with cancer have generally been prioritized for COVID-19 vaccines, protection against

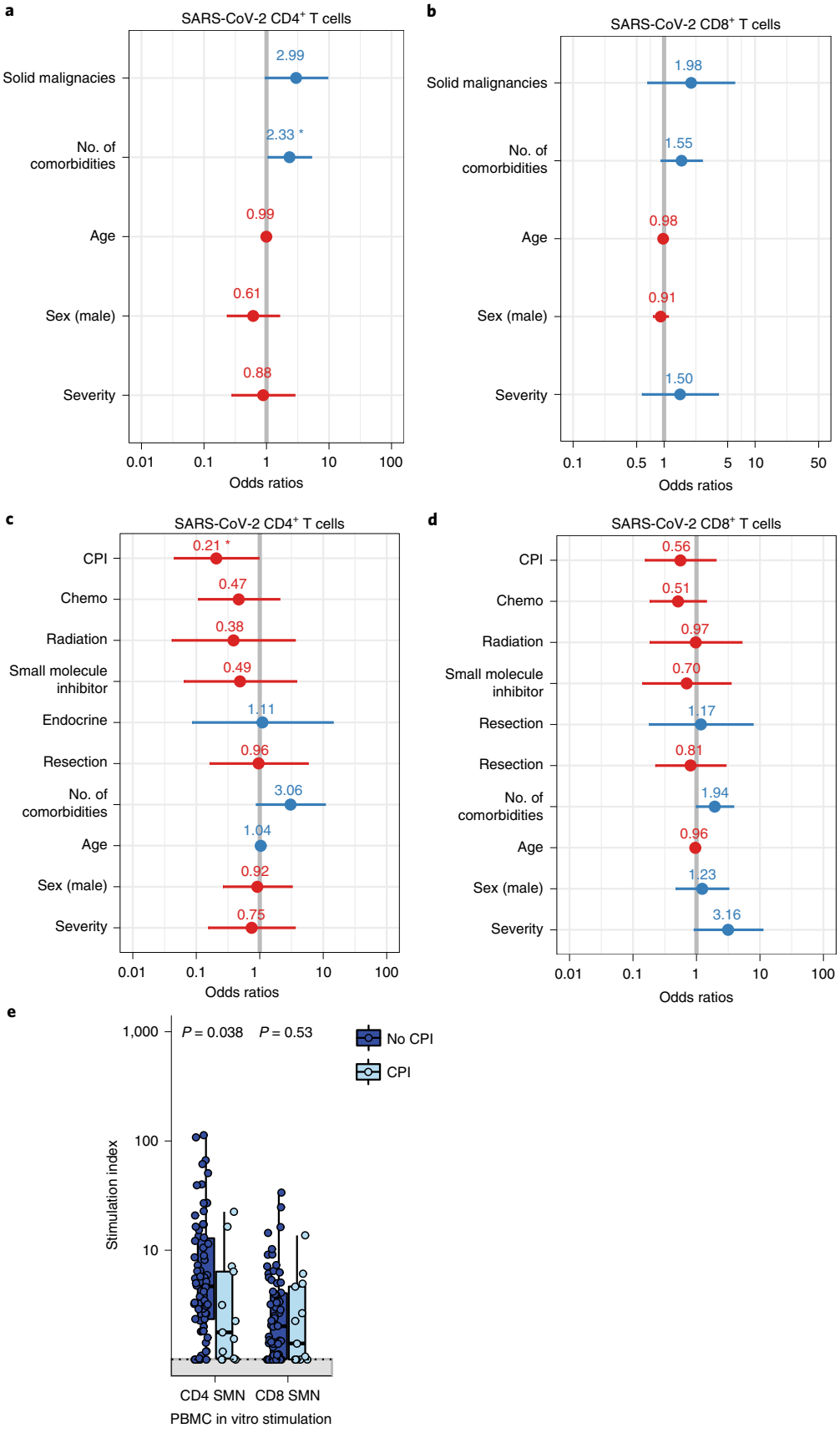

evolving variants is critically relevant in the context of COVID-19-vaccine-induced immunity[29].

During acute SARS-CoV-2 infection, patients with cancer were previously shown to have depleted T cells that showed markers of activation and exhaustion and correlated with COVID-19 severity, but SsT cells were not evaluated[12]. In our cohort, at a median of 54 d POD, SsT cells (including functional IFN-γ-secreting SsT cells) were present in the majority of evaluated patients with solid malignancies (76%) or hematological malignancies (52%). In both the acute phase and the convalescent phase of SARS-CoV-2 infection, a substantial proportion of SARS-CoV-2-specific CD4+ T cells are follicular helper T cells[21,36], which are required for IgG and neutralizing responses by B cells[37]. Accordingly, in our study, the level of CD4+ T cells was significantly correlated with S1-reactive antibody titers in patients with solid tumors, which probably reflected activation of B cells following a follicular helper T cell response. Lack of detectable T cell responses to SARS-CoV-2 was not associated with any cancer-specific factors other than treatment withCPI within 3 months of SARS-CoV-2 infection (in solid tumors). We found that CPI treatment was associated with a lower level of SARS-CoV-2-specific CD4+ T cells but not that of CD8+ T cells. It was previously shown that PD-1 blockade during acute viral infection can increase viral clearance by promoting CD8+ T cell proliferation but can also impair CD8+ T cell memory differentiation, thereby impairing long-term immunity[38]. Although the impact of PD-1 blockade on the CD4+ T cell response to acute infection is less well understood, PD-1 signaling regulates the expansion of CD4+ T cells after an immunogenic stimulus[39], which offers a potential explanation for our finding of lower CD4+ T cell levels. Overall, this finding warrants validation in larger datasets, but this is unlikely to be clinically important, given the lack of consistent association between CPIs and COVID-19 outcomes[5–8].

We found an inverse relationship between antibody responses and SsT cell responses in patients with hematological malignancies, whereby patients with leukemia had more pronounced antibody responses but impaired SsT cell responses, and the opposite was true for patients with lymphoma. Furthermore, we found SsT cells in four of five evaluable patients on anti-CD20 treatment, none of whom had detectable humoral responses. In total, all but one patient with hematological malignancy had mild or moderate COVID-19 disease from which they recovered. This suggests that SsT cell responses, specifically CD8+ T cells and non–spike-specific SsT cells, can at least partially compensate for defective humoral responses. In a recent study, 10 of 13 patients with hematological malignancy and COVID-19 had detectable SsT cells, the levels of which were associated with improved survival (including in those on anti-CD20 therapy)[11]. T cells have been shown to play a crucial role in the clearance of acute SARS-CoV infection in preclinical animal models[40,41], and early induction of functional SsT cells are associated with rapid viral clearance and mild COVID-19 disease in patients without cancer[42]. VOCs are not suspected to escape SsT cell responses, due to their highly multi-antigenic properties[43]. The emerging data from our study and that of others[44] suggest that T cell responses are probably important in those with hematological malignancies and may offer protection from severe COVID-19 in the absence of humoral responses. Notably, SsT cells were shown to be induced by COVID-19 vaccines in both populations without cancer[45,46] and those with cancer[29] and to have activity against VOCs[43]. Overall, our data on natural immunity also bear relevance to vaccination approaches in this population, especially the context of heterologous vaccination that aims to optimally boost humoral and cellular responses[47–49].

This report has several limitations. First, the lack of a broader matched control group without cancer prevents direct comparisons between populations with cancer and those without cancer. Second, as recruitment to CAPTURE commenced in May 2020, which marked the end of the first wave of SARS-CoV-2 infections in the United Kingdom, most of the participants initially recruited were infected prior to study enrollment and were evaluated in the convalescent phase. The fact that we recorded only two COVID-19-related deaths may reflect this, as well as the relatively low proportion of lung and hematological malignancies, which are the two cancer groups with increased COVID-19-related mortality)[3–6]. Furthermore, all but 1 patient with hematological malignancy in our cohort recovered, whereas 11 of 18 patients with blood cancer died due to COVID-19 at our institution[50] before enrollment into CAPTURE commenced. Thus, it is possible that the patients with hematological malignancy in our analysis are not entirely representative of this population. Nevertheless, the cohort as a whole provides a broader representation of all patients with cancer than do those of other studies. Another limitation pertains to our SsT cell evaluation, which was performed at a single time point, and therefore the proportion of patients with a T cell response may be underestimated. Also, although we did not assay against viral peptide pools for other human viruses (such as EBV or CMV), reports suggest that specific patterns of activation markers can be detected on SARS-CoV-2-specific T cells[51]. Finally, our analyses are probably underpowered for robust detection of differences in immune responses between cancer subtypes.

In summary, our data suggest that patients with solid malignancies develop humoral and cellular immunity to SARS-CoV-2, with NAbs detectable for up to 11 months. In line with other reports[11,12], we found that patients with hematological malignancies had impaired humoral responses, and this was associated with disease subtype and anti-CD20 treatment. However, such patients frequently had detectable SsT cell responses. Finally, we found that neutralizing activity against VOCs was reduced in patients infected with WT SARS-CoV-2, which raises concerns about the protection afforded by natural immunity to new SARS-CoV-2 VOCs. Whether such responses can be boosted by COVID-19 vaccines remains under investigation in the vaccine cohort of our study, which includes the currently predominant Delta VOC[29].

Methods

Study design. CAPTURE (NCT03226886) is a prospective, longitudinal cohort study that commenced recruitment in May 2020 at the Royal Marsden NHS Foundation Trust. The study design has been previously published[14]. In brief, adult patients with current or history of invasive cancer are eligible for enrollment (Fig. 1a). Inclusion criteria are intentionally broad and patients are approached irrespective of cancer type, stage or treatment. Patients with confirmed or suspected SARS-CoV-2 infection are targeted with broader recruitment in the course of routine clinical care (asymptomatic cases). Patients are screened at each study visit and classified as SARS-CoV-2-negative or SARS-CoV-2-positive on the basis of a laboratory case definition of RT–PCR-positive result and/or S1-reactive antibodies (details below). The primary end point is to describe the population characteristics of patients with cancer who are positive and negative for SARS-CoV-2. The secondary end points include the impact of COVID-19 on long-term survival and intensive care unit admission rates. Exploratory end points pertain to characterizing clinical and immunological determinants of COVID-19 in patients with cancer.

CAPTURE was approved as a sub-study of TRACERx Renal (NCT03226886). TRACERx Renal was initially approved by the NRES Committee London on 17 January 2012. The TRACERx Renal sub-study CAPTURE was submitted as part of Substantial Amendment 9 and approved by the Health Research Authority on 30 April 2020 and the NRES Committee London on 1 May 2020. CAPTURE is being conducted in accordance with the ethical principles of the Declaration of Helsinki, Good Clinical Practice and applicable regulatory requirements. All patients provided written informed consent to participate.

Study schedule and follow-up. Clinical data and sample collection for participating patients with cancer is performed at baseline and at clinical visits per standard-of-care management during the first year of follow-up; frequency varies depending on in- or outpatient status and systemic anticancer treatment regimens. For inpatients, study assessments are repeated every 2–14 d. For outpatients, the follow-up study assessments are aligned with clinically indicated hospital attendances. The frequency of study assessments in the first year for patients on anticancer therapies are as follows: every cycle for CPIs or targeted therapies; every second cycle for chemotherapy; every outpatient appointment (maximum

6 weekly) for patients on endocrine therapy or in surveillance or routine cancer care follow-up. Patient-reported data are collected 3-monthly via an online questionnaire. In year two to five of follow-up, the frequency of study assessments is reduced (Supplementary Information).

Data and sample sources. Patient-reported outcome data are collected using PROFILES (patient-reported outcomes following initial treatment and long-term evaluation of survivorship; https://profiles-study.rmh.nhs.uk/). PROFILES is a web-based questionnaire administration and management system designed for the study of physical and psychosocial impacts of cancer and its treatment. Online questionnaires for baseline and follow-up assessments were designed to record data for patients with cancer participating in CAPTURE. Collected self-reported data include ethnicity, smoking status, alcohol consumption, recent travel history, occupation, exercise habits, dietary habits, previous medical history, autoimmune disease (self or next of kin), vaccination history, concomitant medication, self-shielding status, previous SARS-CoV-2 tests, SARS-CoV-2 tests in household members and current and recent symptoms. Further demographic, epidemiological and clinical data (such as cancer type, cancer stage and treatment history) are collected from the internal electronic patient record system and entered into detailed case report forms in a secure electronic database. For information on anticancer intervention and response to most recent anticancer intervention, data are collected reflective of the time of SARS-CoV-2 infection as per the definition above, where available or at the time of enrollment if data of disease onset is unknown (for example asymptomatic infections defined by positive serological positivity but negative/no RT–PCR results).

The study samples collected consisted of blood samples, oropharyngeal swabs and archival and excess material from routine clinical investigations. A detailed sampling schedule and methodology has been previously described[14]. Surplus serum from patient biochemistry samples taken as part of routine care were also retrieved and linked to the study IDs before being anonymization and study analysis. Collected data and study samples were de-identified and stored with only the study-specific study identification number. For self-reported data, a PROFILES member number was used, which is generated automatically.

WHO classification of severity of COVID-19. We classified severity of COVID-19 according to the WHO clinical progression scale (0–10)[15]: uninfected, uninfected with no viral RNA detected (0); asymptomatic, viral RNA and/or S1-reactive IgG detected (1); mild (ambulatory), symptomatic and independent (2); symptomatic and assistance needed (3); moderate (hospitalized), no oxygen therapy (if hospitalized for isolation only, record status as for ambulatory patient) (4); oxygen by mask or nasal prongs (5); severe (hospitalized), oxygen by noninvasive ventilation or high flow (6); intubation and mechanical ventilation, $pO_2/F_iO_2 \geq 150$ or $SpO_2/F_iO_2 \geq 200$ (7); mechanical ventilation, $pO_2/F_iO_2 < 150$ ($SpO_2/F_iO_2 < 200$) or vasopressors (8); mechanical ventilation, $pO_2/F_iO_2 < 150$ and vasopressors, dialysis or extracorporeal membrane oxygenation (9); and dead (10).

Cell lines and viruses. SUP-T1 cells stably transfected with spike or control vectors were obtained from M.P. and L.M. Vero E6 cells were obtained from the National Institute for Biological Standards and Control, United Kingdom. The SARS-CoV-2 isolate hCoV-19/England/02/2020 was obtained from the Respiratory Virus Unit, Public Health England, United Kingdom and propagated in Vero E6 cells.

Handling of oronasopharyngeal swabs, RNA isolation and RT–PCR. SARS-CoV-2 RT–PCR was performed from ONP swabs using a diagnostics assay established at the Francis Crick Institute[52]. The complete standard operating procedure is available at https://www.crick.ac.uk/research/covid-19/covid19-consortium. ONP swabs were collected in VTM medium, frozen within 24 h after collection and stored at −80 °C until processing. ONP swabs were handled in a CL3 laboratory inside a biosafety cabinet using appropriate personal protective equipment and safety measures, which were in accordance with a risk assessment and standard operating procedure approved by the safety, health and sustainability committee at the Francis Crick Institute. In brief, 100 µl of swab vial content was inactivated in 5 M guanidinium thiocyanate and RNA isolated using a completely automated kit-free, silica bead-based method.

PCR detection of SARS-CoV-2 was performed from 10 µl extracted RNA using two kits depending on the date of test. Up to 6 December 2020, samples were tested in duplicate using a real-time fluorescent RT–PCR kit for detecting 2019-nCoV (BGI). Positive, negative and extraction controls were included on each plate. Runs were regarded as valid when negative control Ct values were >37 and positive control Ct values were <37. Samples were only considered positive if Ct values in both replicates were <37. From 7 December 2020, tests were performed using a TaqPath COVID-19 CE-IVD RT–PCR kit (Thermo Fisher), this time without replication. Positive and negative controls were included on each plate and samples were reported as positive if 2 or 3 SARS-CoV-2 targets had a Ct value <37 and the internal control Ct < 32. With both kits, samples with non-exponential amplification were excluded from analysis.

Viral sequencing. All PCR-positive samples with ORF1ab Ct value <32 were selected for viral sequencing, representing 52 samples from 32 patients. Sequencing was performed either on Illumina or on Oxford Nanopore Technologies instruments. Oxford Nanopore libraries were prepared following the ARTIC nCoV-2019 sequencing protocol v3 (LoCost) (https://protocols.io/view/ncov-2019-sequencing-protocol-v3-locost-bh42j8ye) and then sequenced for 20 h on a MinION flowcell on a GridION instrument. The ncov2019-artic-nf pipeline (v.1.1.1; https://github.com/connor-lab/ncov2019-artic-nf) written in the Nextflow domain specific language (v.20.10.0)[53] was used to perform quality control, variant calling and consensus sequence generation for the samples. The full command used was 'nextflow run ncov2019-artic-nf–nanopolish–prefix $PREFIX–basecalled_fastq fastq_pass/–fast5_pass fast5_pass/–sequencing_summary sequencing_summary.txt–schemeVersion V3–minReadsPerBarcode 1–minReadsArticGuppyPlex 1 -with-singularity artic-ncov2019-nanopore.img -profile singularity,slurm -r v1.1.1'. Illumina libraries were prepared following the CoronaHiT protocol with minor modifications[54], were pooled, and then were sequenced at 100-bp paired ends on HiSeq 4000. The nf-core/viralrecon pipeline (v.1.1.0)[55] was used to perform quality control, variant calling and consensus sequence generation for the samples. The full command used was 'nextflow run nf-core/viralrecon–input samplesheet.csv–genome 'MN908947.3'–amplicon_bed nCoV-2019.artic.V3.bed–protocol 'amplicon'–callers ivar–skip_assembly–skip_markduplicates–skip_fastqc–skip_picard_metrics–save_align_intermeds -profile crick -r 1.1.0'. Overall, 44 of 52 passed quality control (>50% consensus sequence) and the lineage was obtained using PANGOLIN (https://github.com/cov-lineages/pangolin). In the absence of sequencing data to confirm the causative SARS-CoV-2 variant, all patients tested with Thermo Fisher TaqPath RT–PCR kit that reported S-dropout were considered to be infected with the Alpha VOC.

Viral shedding. Duration of viral shedding was estimated from research and opportunistic swabs and was defined as the time from first positive swab to the last positive swab (preceded by at least one negative swab).

Handling of whole blood samples. All blood samples and isolated products were handled in a CL2 laboratory inside a biosafety cabinet using appropriate personal protective equipment and safety measures in accordance with a risk assessment and standard operating procedure approved by the safety, health and sustainability committee of the Francis Crick Institute. For indicated experiments, serum or plasma samples were heat-inactivated at 56 °C for 30 min before use, after which they were used in a CL1 laboratory.

Plasma and PBMC isolation. Whole blood was collected in EDTA tubes (VWR) and stored at 4 °C until processing. All samples were processed within 24 h. Time of blood draw, processing and freezing was recorded for each sample. Before processing, tubes were brought to room temperature. PBMCs and plasma were isolated by density-gradient centrifugation using pre-filled centrifugation tubes (pluriSelect). Up to 30 ml of undiluted blood was added on top of the sponge and centrifuged for 30 min at 1,000*g* at room temperature. Plasma was carefully removed then centrifuged for 10 min at 4,000*g* to remove debris, then aliquoted and stored at −80 °C. The cell layer was then collected and washed twice in PBS by centrifugation for 10 min at 300*g* at room temperature. PBMCs were resuspended in Recovery cell culture freezing medium (Thermo Fisher Scientific) containing 10% dimethylsulfoxide, placed overnight in CoolCell freezing containers (Corning) at −80 °C and then stored at −80 °C.

Serum isolation. Whole blood was collected in serum coagulation tubes (Vacuette CAT tubes, Greiner) for serum isolation and stored at 4 °C until processing. All samples were processed within 24 h. Time of blood draw, processing and freezing was recorded for each sample. Tubes were centrifuged for 10 min at 2,000*g* at 4 °C. Serum was separated from the clotted portion, aliquoted and stored at −80 °C.

S1-reactive IgG ELISA. Ninety-six-well MaxiSorp plates (Thermo Fisher Scientific) were coated overnight at 4 °C with purified S1 protein in PBS (3 µg ml^{-1} per well in 50 µl) and blocked for 1 h in blocking buffer (PBS, 5% milk, 0.05% Tween 20 and 0.01% sodium azide). Sera were diluted in blocking buffer (1:50 dilution). Fifty microliters of serum were added to the wells and incubated for 2 h at room temperature. After washing four times with PBS-T (PBS and 0.05% Tween 20), plates were incubated with alkaline phosphatase-conjugated goat anti-human IgG (1:1,000 dilution, Jackson ImmunoResearch) for 1 h. Plates were developed by adding 50 µl alkaline phosphatase substrate (Sigma Aldrich) for 15–30 min after six washes with PBS-T. Optical densities were measured at 405 nm on a microplate reader (Tecan). CR3022 (Absolute Antibodies) was used as a positive control. The cutoff for a positive response was defined as the mean negative value × (0.35 × mean positive value).

Flow cytometry for spike-reactive IgG, IgM and IgA. SUP-T1 cells were collected and counted and spike-expressing and control SUP-T1 cells were mixed in a 1:1 ratio. The cell mix was transferred into V-bottom 96-well plates at 20,000 cells per well. Cells were incubated with heat-inactivated serum diluted 1:50 in PBS for 30 min, washed with FACS buffer (PBS, 5% BSA and 0.05% sodium azide) and stained with FITC anti-IgG (clone HP6017, BioLegend), APC anti-IgM (clone MHM-88, BioLegend) and PE anti-IgA (clone IS11-8E10, Miltenyi Biotech)

for 30 min (all antibodies diluted 1:200 in FACS buffer). Cells were washed with FACS buffer and fixed for 20 min in 1% PFA in FACS buffer. Samples were run on a Bio-Rad Ze5 analyzer running Bio-Rad Everest software v.2.4 and analyzed using FlowJo v.10.7.1 (Tree Star) analysis software. Spike-expressing and control SUP-T1 cells were gated and mean fluorescence intensity (MFI) of both populations was measured. MFI in control SUP-T1 cells was subtracted from MFI in spike-expressing SUP-T1 cells and resulting values were divided by MFI in control SUP-T1 cells to calculate the specific increase in MFI. Values >2 were considered positive.

Neutralizing antibody assay against SARS-CoV-2. Confluent monolayers of Vero E6 cells were incubated with SARS-CoV-2 WT or Alpha virus and twofold serial dilutions of heat-treated serum or plasma samples starting at 1:40 for 4 h at 37 °C, 5% CO_2, in duplicate. The inoculum was then removed and cells were overlaid with viral growth medium. Cells were incubated at 37 °C, 5% CO_2. At 24 h after infection, cells were fixed in 4% paraformaldehyde and permeabilized with 0.2% Triton-X-100/PBS. Virus plaques were visualized by immunostaining, as described previously for neutralization of influenza viruses using a rabbit polyclonal anti-NSP8 antibody used at 1:1,000 dilution and anti-rabbit-HRP conjugated antibody at 1:1,000 dilution and detected by action of horseradish peroxidase (HRP) on a tetramethyl benzidine-based substrate. Virus plaques were quantified and half-maximum infective dose was calculated.

High-throughput live virus microneutralization assay. High-throughput live virus microneutralization assays were performed for a subset of 37 patients for WT SARS-CoV-2, Alpha, Beta or Delta. High-throughput live virus microneutralization assays were performed as described previously[56]. Briefly, Vero E6 cells (Institute Pasteur) or Vero E6 cells expressing ACE2 and TMPRSS2 (VAT-1) (Centre for Virus Research)[57] at 90–100% confluency in a 384-well format were first titrated with varying multiplicities of infection of each SARS-CoV-2 variant and varying concentrations of a control monoclonal nanobody to normalize for possible replicative differences between variants and select conditions equivalent to WT virus. Following this calibration, cells were infected in the presence of serial dilutions of patient serum samples. After infection (24 h Vero E6 Pasteur, 16 h VAT-1), cells were fixed with 4% final formaldehyde, permeabilized with 0.2% Triton-X-100 and 3% BSA in PBS (*v*/*v*) and stained for SARS-CoV-2 N protein using Alexa488-labeled-CR3009 antibody produced in-house and cellular DNA using DAPI. Whole-well imaging at 5× was carried out using an Opera Phenix (PerkinElmer) and fluorescent areas and intensity calculated using the Phenix-associated software Harmony 9 (PerkinElmer). Inhibition was estimated from the measured area of infected cells / total area occupied by all cells. The inhibitory profile of each serum sample was estimated by fitting a four-parameter dose–response curve executed in SciPy. Neutralizing antibody titers are reported as the fold-dilution of serum required to inhibit 50% of viral replication (IC_{50}) and are further annotated if they lie above the quantitative (complete inhibition) range, below the quantitative range but still within the qualitative range (partial inhibition is observed but a dose–response curve cannot be fitted because it does not sufficiently span the IC_{50}) or if they show no inhibition at all. IC_{50} values above the quantitative limit of detection of the assay (>25,600) were recoded as 3,000; IC_{50} values below the quantitative limit of the assay (<40) but within the qualitative range were recoded as 39 and data below the qualitative range (no response observed) were recoded as 35.

PBMC stimulation assay. PBMCs for in vitro stimulation were thawed at 37 °C and resuspended in 10 ml of warm complete medium (RPMI and 5% human AB serum) containing 0.02% benzonase. Viable cells were counted and 1×10^6 to 2×10^6 cells were seeded in 200 µl complete medium per well of a 96-well plate. Cells were stimulated with 4 µl per well PepTivator SARS-CoV-2 spike (S), membrane (M) or nucleocapsid (N) pools (synthetic SARS-CoV-2 peptide pools, consisting of 15-mer sequences with 11 amino acid overlap covering the immunodominant parts of the S protein and the complete sequence of the N and membrane M proteins), representing 1 µg ml^{-1} final concentration per peptide (Miltenyi Biotec). SEB (Merck, UK) was used as a positive control at 0.5 µg ml^{-1} final concentration, negative control was PBS containing dimethylsulfoxide at 0.002% final concentration. PBMCs were cultured for 24 h at 37 °C, 5% CO_2.

Activation-induced marker assay. PBMC supernatants were collected for cytokine analysis after stimulation for 24 h. Cells were washed twice in warm PBMCs. Dead cells were stained with 0.5 µl per well Zombie dye V500 for 15 min at room temperature in the dark, then washed once with PBS containing 2% FCS (FACS buffer). A surface staining mix was prepared per well, containing 2 µl per well of each antibody for surface staining in 50:50 brilliant stain buffer (BD) and FACS buffer. PBMCs were stained with 50 µl surface staining mix per well for 30 min at room temperature in the dark. Cells were washed once in FACS buffer and fixed in 1% PFA in FACS buffer for 20 min, then washed once and resuspended in 200 µl PBS. All samples were acquired on a Bio-Rad Ze5 flow cytometer running Bio-Rad Everest software v.2.4 and analyzed using FlowJo v.10.7.1 (Tree Star). Compensation was performed with 20 µl antibody-stained anti-mouse Ig, κ/negative control compensation particle set (BD Biosciences). A total of 1×10^6 live $CD19^-CD14^-$ cells were acquired per sample. Gates were drawn relative to the unstimulated control for each donor. T cell response is displayed as a stimulation index by dividing the percentage of activation-induced marker (AIM)-positive cells by the percentage of cells in the negative control. If negative control was 0, then the minimum value across the cohort was used. When S, M and N stimulation were combined, the sum of AIM-positive cells was divided by three times the percentage of positive cells in the negative control. A 1.5-fold increase in stimulation index was considered positive.

IFN-γ ELISA. IFN-γ ELISA was performed using the human IFN-γ DuoSet ELISA (R&D Systems) according to the manufacturer's instructions. Briefly, 96-well plates were coated overnight with capture antibody, washed twice in wash buffer then blocked with reagent diluent for 2 h at room temperature. Then, 100 µl of PBMC culture supernatants were added and incubated for 1 h at room temperature and washed twice in wash buffer. Following that, 100 µl detection antibody diluted in reagent diluent was added per well and incubated for 2 h at room temperature. Plates were washed twice in wash buffer and 100 µl streptavidin-HRP dilution was added to the plates. Plates were incubated for 20 min in the dark at room temperature and then washed twice in wash buffer. The reaction was developed using 200 µl substrate solution for 20 min in the dark at room temperature then stopped with 50 µl stop solution. Optical density was measured at 450 nm on a multimode microplate reader (Berthold). Serial dilutions of standard were run on each plate. Concentrations were calculated by linear regression of standard concentrations ranging 0–600 pg ml^{-1} and normalized to the number of stimulated PBMC. The assay sensitivity was 5 pg ml^{-1}.

Multiplex immune assay for cytokines and chemokines. The preconfigured multiplex Human Immune Monitoring 65-plex ProcartaPlex immunoassay kit (Invitrogen, Thermo Fisher Scientific) was used to measure 65 protein targets in plasma on the Bio-Plex platform (Bio-Rad Laboratories), using Luminex xMAP technology. Analytes measured included APRIL; BAFF; BLC; CD30; CD40L; ENA-78; eotaxin; eotaxin-2; eotaxin-3; FGF-2; fractalkine; G-CSF; GM-CSF; Gro-α; HGF; IFN-α; IFN-γ; IL-10; IL-12p70; IL-13; IL-15; IL-16; IL-17A; IL-18; IL-1α; IL-1β; IL-2; IL-20; IL-21; IL-22; IL-23; IL-27; IL-2R; IL-3; IL-31; IL-4; IL-5; IL-6; IL-7; IL-8; IL-9; IP-10; I-TAC; LIF; MCP-1; MCP-2; MCP-3; M-CSF; MDC; MIF; MIG; MIP-1α; MIP-1β; MIP-3α; MMP-1; NGF-β; SCF; SDF-1α; TNF-β; TNF-α; TNF-R2; TRAIL; TSLP; TWEAK; and VEGF-A. All assays were conducted as per the manufacturer's recommendation.

Statistics and reproducibility. No statistical method was used to predetermine sample size but as many patients with SARS-CoV-2 infection were recruited as possible, including patients with no history of infection to identify patients in routine care with asymptomatic infection. The experiments were not randomized. The investigators were not blinded to allocation during experiments and outcome assessment.

Data and statistical analysis were performed using FlowJo 10 and R v.3.6.1 in R studio v.1.2.1335. Gaussian distribution of baseline characteristics was tested by Kolmogorov–Smirnov test, and differences in patient groups were compared using chi-squared test, Mann–Whitney test or Kruskal–Wallis test, as appropriate. Statistical methods for each experiment are provided in the figure legends. Gaussian distribution was tested by Kolmogorov–Smirnov test. Mann–Whitney, Wilcoxon, Kruskal–Wallis, chi-squared, Fisher's exact test and Friedman tests were performed for statistical significance. A P value <0.05 was considered significant. The ggplot2 package in R was used for data visualization and illustrative figures were created with BioRender.com. Data were usually plotted as single data points and box plots on a logarithmic scale. For box plots, boxes represent upper and lower quartiles, the line represents the median and whiskers represent 1.5×IQR. Notches represent confidence intervals of the median. For correlation matrix analysis, Spearman rank correlation coefficients were calculated between all parameter pairs using the corrplot package in R without clustering. For pairwise correlation, Spearman rank correlation coefficients were calculated. Multivariate binary logistic regression analysis was performed using the glm function with the stats package in R.

Reporting Summary. Further information on research design is available in the Nature Research Reporting Summary linked to this article.

Data availability

All requests for raw and analyzed data and CAPTURE study protocol will be reviewed by the CAPTURE Trial Management Team, Skin and Renal Clinical Trials Unit, the Royal Marsden NHS Foundation Trust (CAPTURE@rmh.nhs.uk) to determine if the request is subject to confidentiality and data protection obligations. Materials used in this study will be made available upon request. There are restrictions to the availability based on limited quantities. Response to any request for data and/or materials will be given within a 28-d period. Data and materials that can be shared would then be released upon completion of a material transfer agreement. Source data are provided with this paper.

Code availability

No unpublished code was used in this study.

Received: 23 August 2021; Accepted: 17 September 2021;
Published online: 27 October 2021

References

1. Saini, K. S. et al. Mortality in patients with cancer and coronavirus disease 2019: a systematic review and pooled analysis of 52 studies. *Eur. J. Cancer* **139**, 43–50 (2020).
2. Williamson, E. J. et al. Factors associated with COVID-19-related death using OpenSAFELY. *Nature* **584**, 430–436 (2020).
3. Garcia-Suarez, J. et al. Impact of hematologic malignancy and type of cancer therapy on COVID-19 severity and mortality: lessons from a large population-based registry study. *J. Hematol. Oncol.* **13**, 133 (2020).
4. Garassino, M. C. et al. COVID-19 in patients with thoracic malignancies (TERAVOLT): first results of an international, registry-based, cohort study. *Lancet Oncol.* **21**, 914–922 (2020).
5. Lee, L. Y. et al. COVID-19 mortality in patients with cancer on chemotherapy or other anticancer treatments: a prospective cohort study. *Lancet* **395**, 1919–1926 (2020).
6. Kuderer, N. M. et al. Clinical impact of COVID-19 on patients with cancer (CCC19): a cohort study. *Lancet* **395**, 1907–1918 (2020).
7. Grivas, P. et al. Association of clinical factors and recent anticancer therapy with COVID-19 severity among patients with cancer: a report from the COVID-19 and Cancer Consortium. *Ann. Oncol.* **32**, 787–800 (2021).
8. Lee, L. Y. W. et al. COVID-19 prevalence and mortality in patients with cancer and the effect of primary tumour subtype and patient demographics: a prospective cohort study. *Lancet Oncol.* **21**, 1309–1316 (2020).
9. Crolley, V. E. et al. COVID-19 in cancer patients on systemic anti-cancer therapies: outcomes from the CAPITOL (COVID-19 Cancer PatIenT Outcomes in North London) cohort study. *Ther. Adv. Med. Oncol.* **12**, 1758835920971147 (2020).
10. Robilotti, E. V. et al. Determinants of COVID-19 disease severity in patients with cancer. *Nat. Med.* **26**, 1218–1223 (2020).
11. Bange, E. M. et al. CD8$^+$ T cells contribute to survival in patients with COVID-19 and hematologic cancer. *Nat. Med.* **27**, 1280–1289 (2021).
12. Abdul-Jawad, S. et al. Acute immune signatures and their legacies in severe acute respiratory syndrome coronavirus-2 infected cancer patients. *Cancer Cell* **39**, 257–275.e256 (2021).
13. Thakkar, A. et al. Seroconversion rates following COVID-19 vaccination among patients with cancer. *Cancer Cell* **39**, 1081–1090.e2 (2021).
14. Au, L. et al. Cancer, COVID-19, and antiviral immunity: the CAPTURE study. *Cell* **183**, 4–10 (2020).
15. Marshall, J. C. et al. A minimal common outcome measure set for COVID-19 clinical research. *Lancet Infect. Dis.* **20**, e192–e197 (2020).
16. Lowe, K. E., Zein, J., Hatipoglu, U. & Attaway, A. Association of smoking and cumulative pack-year exposure with COVID-19 outcomes in the Cleveland Clinic COVID-19 registry. *JAMA Intern. Med.* **181**, 709–711 (2021).
17. Rosenthal, N., Cao, Z., Gundrum, J., Sianis, J. & Safo, S. Risk factors associated with in-hospital mortality in a US national sample of patients with COVID-19. *JAMA Netw. Open* **3**, e2029058 (2020).
18. Sterlin, D. et al. IgA dominates the early neutralizing antibody response to SARS-CoV-2. *Sci. Transl. Med.* **13**, eabd2223 (2021).
19. Grifoni, A. et al. Targets of T cell responses to SARS-CoV-2 coronavirus in humans with COVID-19 disease and unexposed individuals. *Cell* https://doi.org/10.1016/j.cell.2020.05.015 (2020).
20. Dan, J. M. et al. Immunological memory to SARS-CoV-2 assessed for up to 8 months after infection. *Science* **371**, eabf4063 (2021).
21. Moderbacher, C. R. et al. Antigen-specific adaptive immunity to SARS-CoV-2 in acute COVID-19 and associations with age and disease severity. *Cell* https://doi.org/10.1016/j.cell.2020.09.038 (2020).
22. Weiskopf, D. et al. Phenotype and kinetics of SARS-CoV-2-specific T cells in COVID-19 patients with acute respiratory distress syndrome. *Sci. Immunol.***5**, eabd2071 (2020).
23. Mateus, J. et al. Selective and cross-reactive SARS-CoV-2 T cell epitopes in unexposed humans. *Science* https://doi.org/10.1126/science.abd3871 (2020).
24. Marra, A. et al. Seroconversion in patients with cancer and oncology health care workers infected by SARS-CoV-2. *Ann. Oncol.* **32**, 113–119 (2021).
25. Dispinseri, S. et al. Neutralizing antibody responses to SARS-CoV-2 in symptomatic COVID-19 is persistent and critical for survival. *Nat. Commun.* **12**, 2670 (2021).
26. Earle, K. A. et al. Evidence for antibody as a protective correlate for COVID-19 vaccines. *Vaccine* **39**, 4423–4428 (2021).
27. Khoury, D. S. et al. Neutralizing antibody levels are highly predictive of immune protection from symptomatic SARS-CoV-2 infection. *Nat. Med.* **27**, 1205–1211 (2021).
28. Ju, B. et al. Human neutralizing antibodies elicited by SARS-CoV-2 infection. *Nature* **584**, 115–119 (2020).
29. Fendler, A. et al. Adaptive immunity and neutralizing antibodies against SARS-CoV-2 variants of concern following vaccination in patients with cancer: the CAPTURE study. *Nat. Cancer* https://doi.org/10.1038/s43018-021-00274-w (2021).
30. Seow, J. et al. Longitudinal observation and decline of neutralizing antibody responses in the three months following SARS-CoV-2 infection in humans. *Nat. Microbiol.* **5**, 1598–1607 (2020).
31. Gaebler, C. et al. Evolution of antibody immunity to SARS-CoV-2. *Nature* **591**, 639–644 (2021).
32. Wang, Z. et al. Naturally enhanced neutralizing breadth against SARS-CoV-2 one year after infection. *Nature* **595**, 426–431 (2021).
33. Achiron, A. et al. Humoral immune response to COVID-19 mRNA vaccine in patients with multiple sclerosis treated with high-efficacy disease-modifying therapies. *Ther. Adv. Neurol. Disord.* https://doi.org/10.1177/17562864211012835 (2021).
34. Garcia-Beltran, W. F. et al. COVID-19 neutralizing antibodies predict disease severity and survival. *Cell* **184**, 476–488.e11 (2021).
35. Vacharathit, V. et al. CoronaVac induces lower neutralising activity against variants of concern than natural infection. *Lancet Infect. Dis.* **21**, 1352–1354 (2021).
36. Juno, J. A. et al. Humoral and circulating follicular helper T cell responses in recovered patients with COVID-19. *Nat. Med.* **26**, 1428–1434 (2020).
37. Murugesan, K. et al. Interferon-γ release assay for accurate detection of severe acute respiratory syndrome coronavirus 2 T-cell response. *Clin. Infect. Dis.* https://doi.org/10.1093/cid/ciaa1537 (2020).
38. Pauken, K. E. et al. The PD-1 pathway regulates development and function of memory CD8$^+$ T cells following respiratory viral infection. *Cell Rep.* **31**, 107827 (2020).
39. Konkel, J. E. et al. PD-1 signalling in CD4$^+$ T cells restrains their clonal expansion to an immunogenic stimulus, but is not critically required for peptide-induced tolerance. *Immunology* **130**, 92–102 (2010).
40. Zhao, J., Zhao, J. & Perlman, S. T cell responses are required for protection from clinical disease and for virus clearance in severe acute respiratory syndrome coronavirus-infected mice. *J. Virol.* **84**, 9318–9325 (2010).
41. Muñoz-Fontela, C. et al. Animal models for COVID-19. *Nature* **586**, 509–515 (2020).
42. Tan, A. T. et al. Early induction of functional SARS-CoV-2-specific T cells associates with rapid viral clearance and mild disease in COVID-19 patients. *Cell Rep.* **34**, 108728 (2021).
43. Tarke, A. et al. Impact of SARS-CoV-2 variants on the total CD4$^+$ and CD8$^+$ T cell reactivity in infected or vaccinated individuals. *Cell Rep. Med.* https://doi.org/10.1016/j.xcrm.2021.100355 (2021).
44. Apostolidis, S.A. et al. Cellular and humoral immune responses following SARS-CoV-2 mRNA vaccination in patients with multiple sclerosis on anti-CD20 therapy. *Nat. Med.* https://doi.org/10.1038/s41591-021-01507-2 (2021).
45. Sahin, U. et al. COVID-19 vaccine BNT162b1 elicits human antibody and T_H1 T cell responses. *Nature* **586**, 594–599 (2020).
46. Ewer, K. J. et al. T cell and antibody responses induced by a single dose of ChAdOx1 nCoV-19 (AZD1222) vaccine in a phase 1/2 clinical trial. *Nat. Med.* **27**, 270–278 (2021).
47. Normark, J. et al. Heterologous ChAdOx1 nCoV-19 and mRNA-1273 vaccination. *N. Engl. J. Med.* **385**, 1049–1051 (2021).
48. Barros-Martins, J. et al. Immune responses against SARS-CoV-2 variants after heterologous and homologous ChAdOx1 nCoV-19/BNT162b2 vaccination. *Nat. Med.* **27**, 1525–1529 (2021).
49. Spencer, A.J. et al. Heterologous vaccination regimens with self-amplifying RNA and adenoviral COVID vaccines induce robust immune responses in mice. *Nat. Commun.* **12**, 2893 (2021).
50. Angelis, V. et al. Defining the true impact of coronavirus disease 2019 in the at-risk population of patients with cancer. *Eur. J. Cancer* **136**, 99–106 (2020).
51. Sekine, T. et al. Robust T cell immunity in convalescent individuals with asymptomatic or mild COVID-19. *Cell* **183**, 158–168 (2020).
52. Aitken, J. et al. Scalable and robust SARS-CoV-2 testing in an academic center. *Nat. Biotechnol.* **38**, 927–931 (2020).
53. Di Tommaso, P. et al. Nextflow enables reproducible computational workflows. *Nat. Biotechnol.* **35**, 316–319 (2017).
54. Baker, D. J. et al. CoronaHiT: high-throughput sequencing of SARS-CoV-2 genomes. *Genome Med.* **13**, 21 (2021).
55. Ewels, P. A. et al. The nf-core framework for community-curated bioinformatics pipelines. *Nat. Biotechnol.* **38**, 276–278 (2020).
56. Faulkner, N. et al. Reduced antibody cross-reactivity following i nfection with B.1.1.7 than with parental SARS-CoV-2 strains. *eLife* **10**, e69317 (2021).
57. Rihn, S. J. et al. A plasmid DNA-launched SARS-CoV-2 reverse genetics system and coronavirus toolkit for COVID-19 research. *PLoS Biol.* **19**, e3001091 (2021).

Acknowledgements

We thank the CAPTURE trial team, including E. Carlyle, K. Edmonds and L. Del Rosario, as well as S. Agarwal, H. Ahmod, N. Ash, R. Dhaliwal, L. Dowdie, T. Foley, L. Holt, D. Kabir, M. O'Flaherty, M. Ndlovu, S. Ali, J. Korteweg, C. Lewis, K. Lingard, M. Mangwende, A. Murra, K. Peat, S. Sarker, N. Shaikh, S. Vaughan and F. Williams. We acknowledge support from the clinical and research teams at participating units at the Royal Marsden Hospital, including E. Black, A. Dela Rosa, C. Pearce, J. Bazin, L. Conneely, C. Burrows, T. Brown, J. Tai, E. Lidington, H. Hogan, A. Upadhyay, D. Capdeferro, I. Potyka, A. Drescher, F. Baksh, M. Balcorta, C. Da Costa Mendes, J. Amorim, V. Orejudos and L. Davison. We also thank volunteer staff at the Francis Crick Institute and the Crick COVID-19 Consortium and A. Lilley for help with neutralizing assays, A. Toncheva and staff at the cloning unit at Autolus, including J. Sillibourne, K. Ward, K. Lamb and P. Wu. We thank B. Stockinger for thoughtful review and comments on the manuscript. Due to the pace at which the field is evolving, we acknowledge researchers in COVID-19, particularly in furthering our understanding of SARS-CoV-2 infection and we apologize for work that was not cited. This research was funded in part, by the Cancer Research UK (grant no. C50947/A18176). This work was supported by the Francis Crick Institute, which receives its core funding from Cancer Research UK (CRUK) (FC001988, FC001218, FC001099, FC001002, FC001078, FC001169 and FC001030), the UK Medical Research Council (FC001988, FC001218, FC001099, FC001002, FC001078, FC001169 and FC001030) and the Wellcome Trust (FC001988, FC001218, FC001099, FC001002, FC001078, FC001169 and FC001030). For the purpose of Open Access, the author has applied a CC BY public copyright license to any Author Accepted Manuscript version arising from this submission. TRACERx Renal is partly funded by the National Institute for Health Research (NIHR) Biomedical Research Centre (BRC) at the Royal Marsden Hospital and Institute of Cancer Research (A109). The CAPTURE study is sponsored by the Royal Marsden NHS Foundation Trust and funded from a grant from the Royal Marsden Cancer Charity. A.F. has received funding from the European Union's Horizon 2020 Research and Innovation program under Marie Skłodowska-Curie grant no. 892360. L.A. is funded by the Royal Marsden Cancer Charity. S.T. is funded by CRUK (grant no. A29911); the Francis Crick Institute, which receives its core funding from CRUK (FC10988), the UK Medical Research Council (FC10988) and the Wellcome Trust (FC10988); the NIHR BRC at the Royal Marsden Hospital and Institute of Cancer Research (grant no. A109), the Royal Marsden Cancer Charity, the Rosetrees Trust (grant no. A2204), Ventana Medical Systems (grant nos. 10467 and 10530), the National Institute of Health (U01 CA247439) and Melanoma Research Alliance (award no. 686061). C. Swanton is a Royal Society Napier Research Professor (RP150154). His work is supported by the Francis Crick Institute, which receives its core funding from CRUK (FC001169), the UK Medical Research Council (FC001169) and the Wellcome Trust (FC001169). C. Swanton is funded by the CRUK (TRACERx, PEACE and CRUK Cancer Immunotherapy Catalyst Network), CRUK Lung Cancer Centre of Excellence, the Rosetrees Trust, Butterfield and Stoneygate Trusts, NovoNordisk Foundation (ID16584), Royal Society Research Professorship Enhancement Award (RP/EA/180007), the NIHR BRC at University College London Hospitals, the CRUK-UCL Centre, Experimental Cancer Medicine Centre and the Breast Cancer Research Foundation, USA. His research is supported by a Stand Up To Cancer (SU2C)-LUNGevity-American Lung Association Lung Cancer Interception Dream Team Translational Research Grant (SU2C-AACR-DT23-17). SU2C is a program of the Entertainment Industry Foundation. Research grants are administered by the American Association for Cancer Research, the Scientific Partner of SU2C. C. Swanton also receives funding from the European Research Council under the European Union's Seventh Framework Programme (FP7/2007-2013) Consolidator Grant (FP7-THESEUS-617844), European Commission ITN (FP7-PloidyNet 607722), an ERC Advanced Grant (PROTEUS) from the European Research Council under the European Union's Horizon 2020 Research and Innovation program (835297) and Chromavision from the European Union's Horizon 2020 Research and Innovation program (665233). R.W. has received Francis Crick Institute support from the Wellcome Trust (FC0010218), UKRI (FC0010218), CRUK (FC0010218) and research funding from the Wellcome Trust (203135 and 222754), Rosetrees Trust (M926) and the South African Medical Research Council.

Author contributions

S.T., L.A. and L.A.B. were responsible for conceptualization of the study. Methodology was developed by S.T., A.F., F.B., K.A.W., G.K. and R.H. M.G. was responsible for software. Formal analysis was conducted by A.F., L.A., S.T.C.S., G.K., K.A.W., R.J.W., R.H. and M.C. Investigations were conducted by A.F., L.A., F.B., S.T.C.S, B.S., C.G., W.X., B.W., K.A.W., M.C., A.A-D. and R.H. Resources were provided by S.T., A.F., L.A., L.A.B., F.B., S.T.C.S., B.S., C.G., B.W., W.X., M.C., G.C., M.P., L.M., R.S., C.G., H.F., M.G., F.G., O.C., T.S., Y.K., Z.T. and I.L. Data were curated by L.A.B., S.T.C.S., B.S., C.G., A.F. and L.A. Writing of the original draft was the responsibility of S.T., K.R., A.F., L.A. and S.T.C.S.; A.F., L.A., S.T.C.S., F.B., M.C., L.A.B., K.R., W.G., B.S., C.L.G., B.W., W.X., A.M.S., N.J.-H., G.H.C., M.P., L.M., K.W.N, E.C., K.E., L.D.R., S.S., K.L., M.M., L.H., H.A., R.S., C.G., H.R.F., A.A.-D., P.H., S.C., M.H., M.W., R.G., M.C., L.C., H.P., M.G., E.N., A.-S., J.I.M., J.N., F.G., R.L.S., C.M., D.C., I.C., N.S., N.T., L.W., N.v.A., R.L.J., J.D., S. Banerjee, K.C.T., S.J., M.O'B., O.C., K.H., S.B., J.B., A. Robinson, C. Stephenson, T.S., Y.K., Z.T., I.L., S.G., A.O., A. Reid, K.Y., A.J.S.F., L.P., S. Gandhi, S. Gamblin, C. Swanton, E.N., S.K., N.Y., K.A.W., A.S., R.H., G.K., J.L., R.J.W. and S.T. were responsible for review and editing of the manuscript. Visualization was carried out by A.F., S.T.C.S., S.T. and L.A. Supervision was conducted by S.T. Trial conduct was overseen by S.T., L.A., S.T.C.S., E.C., L.R., K.E., L.A.B., J.L., N.Y., A.R., E.N. and S.K.

Competing interests

S.T. has received speaking fees from Roche, AstraZeneca, Novartis and Ipsen. S.T. has the following patents filed: Indel mutations as a therapeutic target and predictive biomarker PCTGB2018/051892 and PCTGB2018/051893 and Clear Cell Renal Cell Carcinoma Biomarkers P113326GB. N.Y. has received conference support from Celegene. A.R. received speaker's fees from Janssen and AstraZeneca; travel support from Janssen and Astellas, and consultancy fees from AstraZeneca. D.C. received funding from MedImmune, AstraZeneca, Clovis, Eli Lilly, 4SC, Bayer, Celgene and Roche, and is on the advisory board of OVIBIO. J.L. has received research funding from Bristol-Myers Squibb, Merck, Novartis, Pfizer, Achilles Therapeutics, Roche, Nektar Therapeutics, Covance, Immunocore, Pharmacyclics and Aveo, and served as a consultant to Achilles, Astra Zeneca, Boston Biomedical, Bristol-Myers Squibb, Eisai, EUSA Pharma, GlaxoSmithKline, Ipsen, Imugene, Incyte, iOnctura, Kymab, Merck Serono, Nektar, Novartis, Pierre Fabre, Pfizer, Roche Genentech, Secarna and Vitaccess. I.C. has served as a consultant to Eli-Lilly, Bristol Meyers Squibb, MSD, Bayer, Roche, Merck Serono, Five Prime Therapeutics, Astra Zeneca, OncXerna, Pierre Fabre, Boehringer-Ingelheim, Incyte, Astella, GSK, Sotio and, Eisai; has received research funding from Eli-Lilly & Janssen-Cilag; and has received honorarium from Eli-Lilly, Eisai, Servier. A.O. acknowledges receipt of research funding from Pfizer and Roche; speakers fees from Pfizer, Seagen, Lilly and Astra Zeneca; is an advisory board member of Roche, Seagen and Astra Zeneca; and has received conference support from Leo Pharmaceuticals, Astra Zeneca/Diachi-Sankyo and Lilly. C. Swanton acknowledges grant support from Pfizer, Astra Zeneca, Bristol-Myers Squibb, Roche-Ventana, Boehringer-Ingelheim, Archer Dx (collaboration in minimal residual disease sequencing technologies) and Ono Pharmaceutical; is an Astra Zeneca Advisory Board member and Chief Investigator for the MeRmaiD1 clinical trial; has consulted for Amgen, Pfizer, Novartis, GlaxoSmithKline, MSD, Bristol-Myers Squibb, Celgene, Astra Zeneca, Illumina, Genentech, Roche-Ventana, GRAIL, Medicxi, Metabomed, Bicycle Therapeutics and the Sarah Cannon Research Institute; has stock options in Apogen Biotechnologies, Epic Bioscience, GRAIL and has stock options; and is co-founder of Achilles Therapeutics. C. Swanton holds European patents relating to assay technology to detect tumor recurrence (PCT/GB2017/053289); to targeting neoantigens (PCT/EP2016/059401), identifying patent response to immune-checkpoint blockade (PCT/EP2016/071471), determining HLA LOH (human leukocyte antigen loss of heterozygosity) (PCT/GB2018/052004), predicting survival rates of patients with cancer (PCT/GB2020/050221), identifying patients who respond to cancer treatment (PCT/GB2018/051912), a US patent relating to detecting tumor mutations (PCT/US2017/28013) and both a European and US patent related to identifying insertion/deletion mutation targets (PCT/GB2018/051892). L.P. has received research funding from Pierre Fabre and honoraria from Pfizer, Ipsen, Bristol-Myers Squibb and EUSA Pharma. S.B. has received institutional research funding from AstraZeneca, Tesaro, GSK; speakers fees from Amgen, Pfizer, Astra Zeneca, Tesaro, GSK, Clovis, Takeda, Immunogen and Mersana; and has an advisory role for Amgen, AstraZeneca, Epsilogen, Genmab, Immunogen, Mersana, Merck Sharp & Dohme, Merck Serono, Oncxerna, Pfizer and Roche. N.T. has received advisory board honoraria from AstraZeneca, Bristol-Myers Squibb, Lilly, Merck Sharpe and Dohme, Novartis, Pfizer, Roche/Genentech, GlaxoSmithKline, Zentalis Pharmaceuticals, Repare Therapeutics and Arvinas; and research funding from AstraZeneca, BioRad, Pfizer, Roche/Genentech, Merck Sharpe & Dohme, Guardant Health, Invitae, Inivata, Personalis and Natera. M.O.B. is on advisory boards for Amgen, Pierre Fabre, Pharmamar, Puma, MSD and Roche. A.M.S. received and educational grant from Janssen-Cilag. N.S. received travel grants from AstraZeneca, BMS, Eli Lilly, Merck, Roche and MSD Oncology; received honoraria from Eli Lilly, Merck Serono, MSD Oncology, Pierre Fabre, Servier, GSK and Amgen; and is on the advisory board for Pfizer, AstraZeneca, Servier and MSD. N.S. received funding from AstraZeneca, BMS, Pfizer, NIHR EME, RMCC and RM/ICR BCR. R.L.J. received research support from Merck Sharp & Dohme and GSK; and received consultation fees from Adaptimmune, Astex, Athenex, Bayer, Boehringer Ingelheim, Blueprint, Cinigen, Eisai, Epizyme, Daichii, Deciphera, Immundesign, Immunicum, Karma Oncology, Lilly, Merck, Mundipharma, Pharmamar, Springworks, SynOx, Tracon, Upto Date and Merck Sharp & Dohme. A.F., L.A., S.T.C.S., F.B., M.C., L.A.B., K.R., W.G., B.S., C.L.G., B.W., W.X., N.J.-H., G.H.C., M.P., L.M., K.W.N., E.C., K.E., L.D.R., S.S., K.L., M.M., L.H., H.A., R.S., C.G., H.R.F., A.A.-D., P.H., S.C., M.H., M.W., R.G., M.C., L.C., H.P., M.G., E.N., A.-S., J.I.M., J.N., F.G., R.L.S., C.M., D.C. L.W., N.v.A., J.D., K.C.T., S.J., O.C., K.H., S.B., J.B., A. Robinson, C. Stephenson, T.S., Y.K., Z.T., I.L., S.G., A.O., A. Reid, K.Y., A.J.S.F., S. Gamblin, C. Swanton, E.N., S.K., K.A.W., A.S., R.H., G.K. and R.J.W. declare no competing interests.

Additional information

Extended data is available for this paper at https://doi.org/10.1038/s43018-021-00275-9.

Supplementary information The online version contains supplementary material available at https://doi.org/10.1038/s43018-021-00275-9.

Correspondence and requests for materials should be addressed to Samra Turajlic.

Peer review information *Nature Cancer* thanks Ailong Huang, Sean Lim and the other, anonymous, reviewer(s) for their contribution to the peer review of this work.

Reprints and permissions information is available at www.nature.com/reprints.

[1]Cancer Dynamics Laboratory, The Francis Crick Institute, London, UK. [2]Skin and Renal Units, The Royal Marsden NHS Foundation Trust, London, UK. [3]Tuberculosis Laboratory, The Francis Crick Institute, London, UK. [4]Department of Infectious Disease, Imperial College London, London, UK. [5]Retroviral Immunology Laboratory, The Francis Crick Institute, London, UK. [6]Department of Haematology, University College London Cancer Institute, London, UK. [7]Autolus Ltd., London, UK. [8]Experimental Histopathology Laboratory, The Francis Crick Institute, London, UK. [9]Mass Spectrometry Proteomics Science Technology Platform, The Francis Crick Institute, London, UK. [10]Flow Cytometry Scientific Technology Platform, The Francis Crick Institute, London, UK. [11]Safety, Health and Sustainability, The Francis Crick Institute, London, UK. [12]High Throughput Screening Laboratory, The Francis Crick Institute, London, UK. [13]Advanced Sequencing Facility, The Francis Crick Institute, London, UK. [14]Department of Bioinformatics and Biostatistics, The Francis Crick Institute, London, UK. [15]Scientific Computing Scientific Technology Platform, The Francis Crick Institute, London, UK. [16]Metabolomics Scientific Technology Platform, The Francis Crick Institute, London, UK. [17]Department of Pathology, The Royal Marsden NHS Foundation Trust, London, UK. [18]Translational Cancer Biochemistry Laboratory, The Institute of Cancer Research, London, UK. [19]Department of Radiology, The Royal Marsden NHS Foundation Trust, London, UK. [20]Gastrointestinal Unit, The Royal Marsden NHS Foundation Trust, London and Surrey, London, UK. [21]Breast Unit, The Royal Marsden NHS Foundation Trust, London, UK. [22]Breast Cancer Now Toby Robins Breast Cancer Research Centre, The Institute of Cancer Research, London, UK. [23]Neuro-oncology Unit, The Royal Marsden NHS Foundation Trust, London, UK. [24]Clinical Oncology Unit, The Royal Marsden NHS Foundation Trust, London, UK. [25]Sarcoma Unit, The Royal Marsden NHS Foundation Trust and Institute of Cancer Research, London, UK. [26]Palliative Medicine, The Royal Marsden NHS Foundation Trust, London, UK. [27]Gynaecology Unit, The Royal Marsden NHS Foundation Trust, London, UK. [28]Anaesthetics, Perioperative Medicine and Pain Department, The Royal Marsden NHS Foundation Trust, London, UK. [29]Department of Surgery and Cancer, Imperial College London, London, UK. [30]Lung Unit, The Royal Marsden NHS Foundation Trust, London, UK. [31]Head and Neck Unit, The Royal Marsden NHS Foundation Trust, London, UK. [32]Targeted Therapy Team, The Institute of Cancer Research, London, UK. [33]Haemato-oncology Unit, The Royal Marsden NHS Foundation Trust, London, UK. [34]Acute Oncology Service, The Royal Marsden NHS Foundation Trust, London, UK. [35]Department of Medical Oncology, Guy's Hospital, London, UK. [36]Uro-oncology Unit, The Royal Marsden NHS Foundation Trust, Surrey, UK. [37]Neurodegeneration Biology Laboratory, The Francis Crick Institute, London, UK. [38]UCL Queen Square Institute of Neurology, London, UK. [39]Structural Biology of Disease Processes Laboratory, The Francis Crick Institute, London, UK. [40]Cancer Evolution and Genome Instability Laboratory, The Francis Crick Institute, London, UK. [41]University College London Cancer Institute, London, UK. [42]Wellcome Center for Infectious Disease Research in Africa, University Cape Town, Cape Town, Republic of South Africa. [43]Division of Genetics and Epidemiology and Division of Breast Cancer Research, The Institute of Cancer Research, London, UK. [44]Worldwide Influenza Centre, The Francis Crick Institute, London, UK. [45]These authors contributed equally: A. Fendler, L. Au, S.T.C. Shepherd. *Lists of authors and their affiliations appear at the end of the paper.
✉e-mail: samra.turajlic@crick.ac.uk

The Crick COVID-19 Consortium

Helen R. Flynn[9], Simon Caidan[11], Michael Howell[12], Mary Wu[12], Robert Goldstone[13], Margaret Crawford[13], Laura Cubitt[13], James I. MacRae[16], Jerome Nicod[13], Sonia Gandhi[37,38], Steve Gamblin[39], Charles Swanton[40,41] and George Kassiotis[5]

A full list of members appears in the Supplementary Information.

The CAPTURE consortium

Annika Fendler[1,45], Lewis Au[1,2,45], Scott T. C. Shepherd[1,2,45], Fiona Byrne[1], Laura Amanda Boos[2], Benjamin Shum[1,2], Camille L. Gerard[1], Andreas M. Schmitt[2], Christina Messiou[19], David Cunningham[20], Ian Chau[20], Naureen Starling[20], Nicholas Turner[21,22], Liam Welsh[23], Robin L. Jones[25], Joanne Droney[26], Susana Banerjee[27], Kate C. Tatham[28,29], Shaman Jhanji[28], Kevin Harrington[31,32], Alicia Okines[21,34], Alison Reid[36], Kate Young[2], Andrew J. S. Furness[2], Lisa Pickering[2], Emma Nicholson[33], Sacheen Kumar[20], Nadia Yousaf[30,34], Katalin A. Wilkinson[3,42], Anthony Swerdlow[43], George Kassiotis[5], James Larkin[2], Robert J. Wilkinson[3,4,42] and Samra Turajlic[1,2]

A full list of members appears in the Supplementary Information.

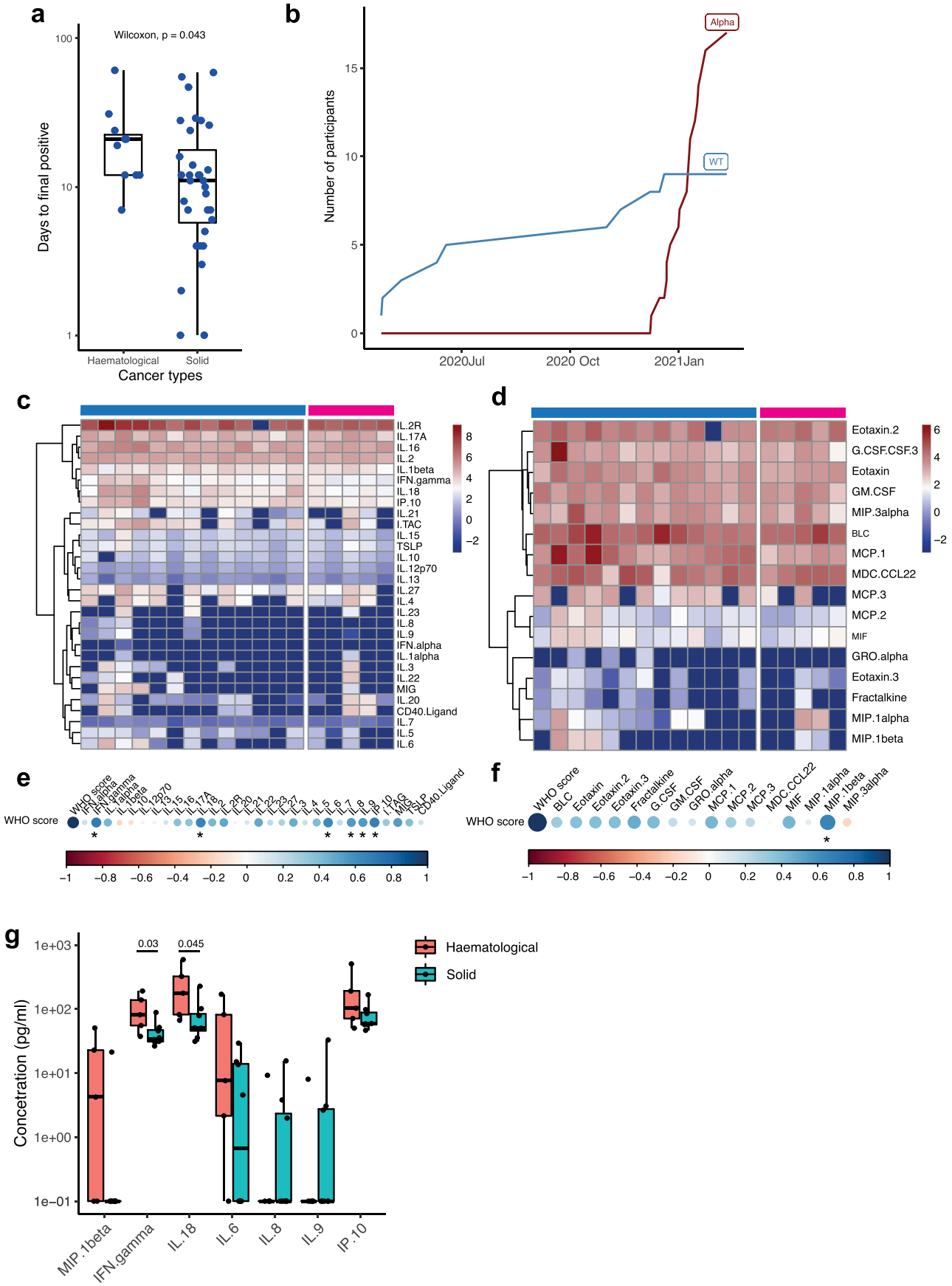

Extended Data Fig. 1 | See next page for caption.

Extended Data Fig. 1 | Duration of viral shedding and SARS-CoV-2 viral strain incidence in the CAPTURE cohort, and cyto/chemokine correlations with COVID-19 severity. a) Duration to final positive swab in patients with solid (n = 32) vs haematological malignancies (n = 11). Boxes indicate the 25 and 75 percentiles, line indicates the median, and whiskers indicate the 10 and 90 percentiles. Dots represent individual samples. Significance was tested by two-sided Wilcoxon Mann-Whitney U test, $p < 0.05$ was considered significant. **b)** Change over time in the dominant SARS-CoV-2 strain as assessed in 44 patients with cancer with viral sequencing data. Cytokine levels related to c) T-cell and d) macrophage responses were measured in patients with cancer with acute SARS-CoV infection (blue bar, n = 13) using the human immune monitoring 65-plex ProcartaPlex immunoassay in serum samples. Samples were measured in duplicates. Control samples are sera from non-matched patients with cancer (pink bar, n = 5) without SARS-CoV-2 infection. Data are presented as the log10 of the concentration in pg ml−1. Correlation of cyto/chemokines related to **e)** T cells and **f)** macrophages with COVID-19 WHO severity score. **g)** Comparisons of cytokine levels between patients with haematological (orange, n = 8) and solid malignancies (aqua, n = 5). Boxes indicate the 25th and 75th percentiles, line indicates the median, and whiskers indicate the 10 and 90 percentiles. Dots represent individual samples. Significance was tested by Wilcoxon-Mann-Whitney U test, p-values are denoted in the graph.

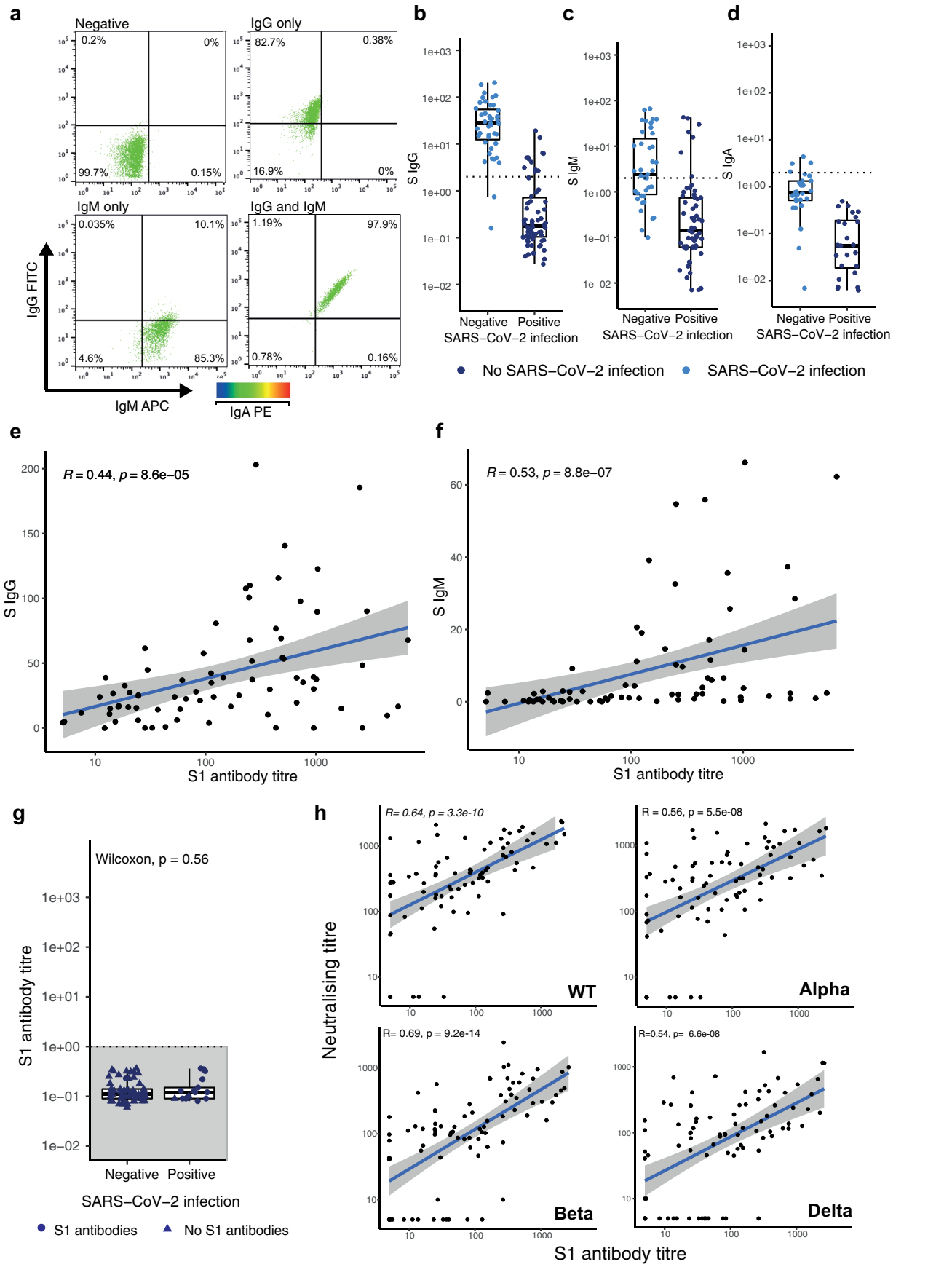

Extended Data Fig. 2 | See next page for caption.

Extended Data Fig. 2 | Spike-reactive and neutralising antibody titers. a) Flow cytometric assays to quantify S-reactive IgG and IgM and IgA levels in sera of patients (n = 109 for IgG and IgM, n = 51 for IgA) with S-reactive antibodies. **b)** S-reactive IgG, **c)** IgM, and **d)** IgA in SARS-CoV-2 positive compared with infection-naive patients (n = 40). Boxes indicate the 25 and 75 percentiles, line indicates the median, and whiskers indicate the 10th and 90th percentiles. **e)** Correlation between S1-reactive IgG and S1-reactive AbT in 40 patients and **f)** Correlation between S1-reactive IgM and S1-reactive AbT in 40 patients. Blue line denotes linear regression line with grey areas marking the 95% confidence band. Regression coefficient and p-values were computed by two-sided spearman regression, $p < 0.05$ was considered significant. **g)** S1-reactive antibodies in pre-pandemic sera of patients (n = 77). Boxes indicate the 25 and 75 percentiles, line indicates the median, and whiskers indicate the 10th and 90th percentiles. **h)** Correlation between NAbT against WT, Alpha, Beta, Delta and S1-reactive AbT in 112 patients. Blue line denotes linear regression line with grey areas marking the 95% confidence band. Regression coefficient and p-values were computed by two-sided spearman regression, $p < 0.05$ was considered significant.

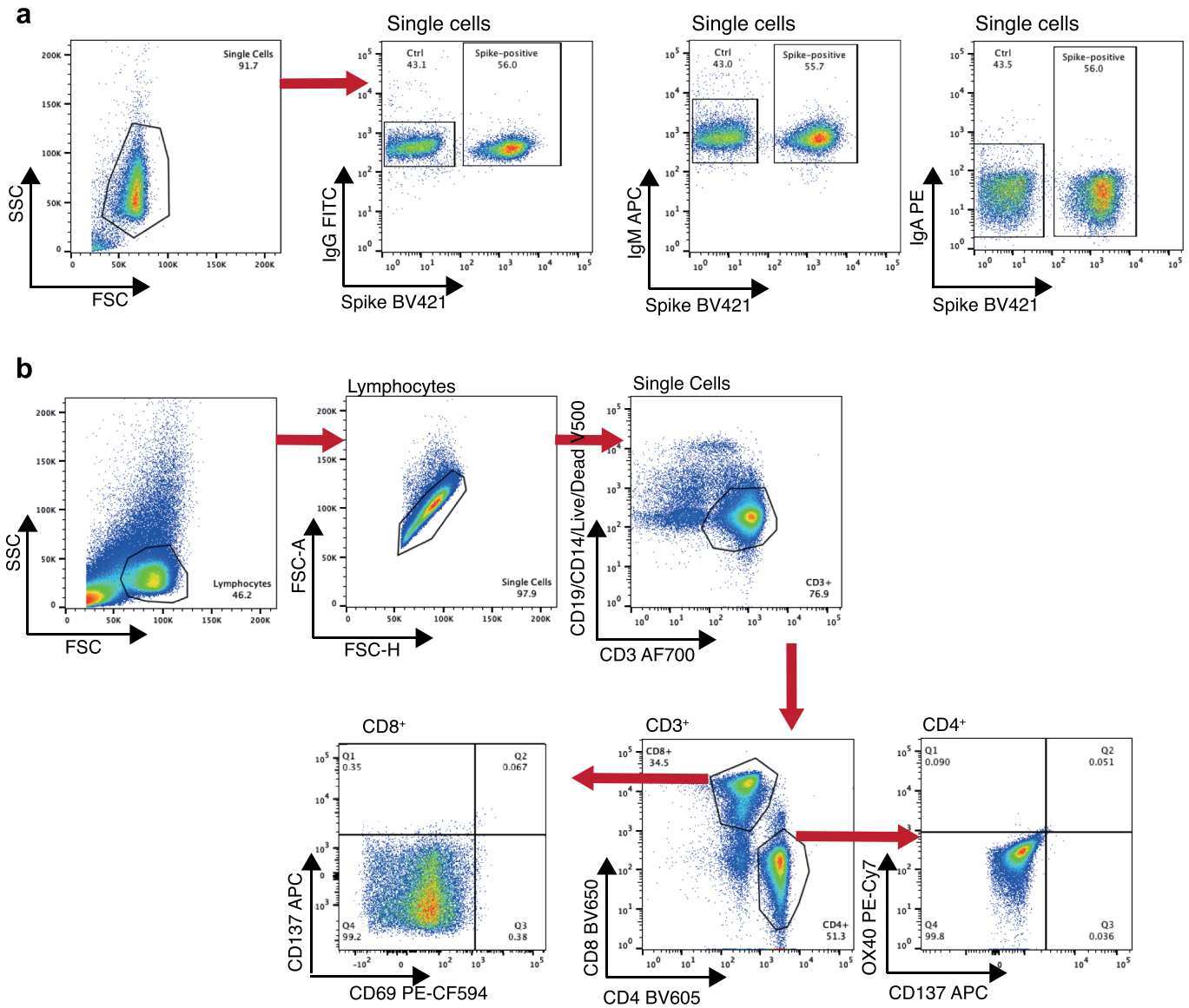

Extended Data Fig. 3 | Gating strategy. Gating strategy for flow analysis of **a**) S-reactive IgG, IgG, IgA and **b**) AIM assay.

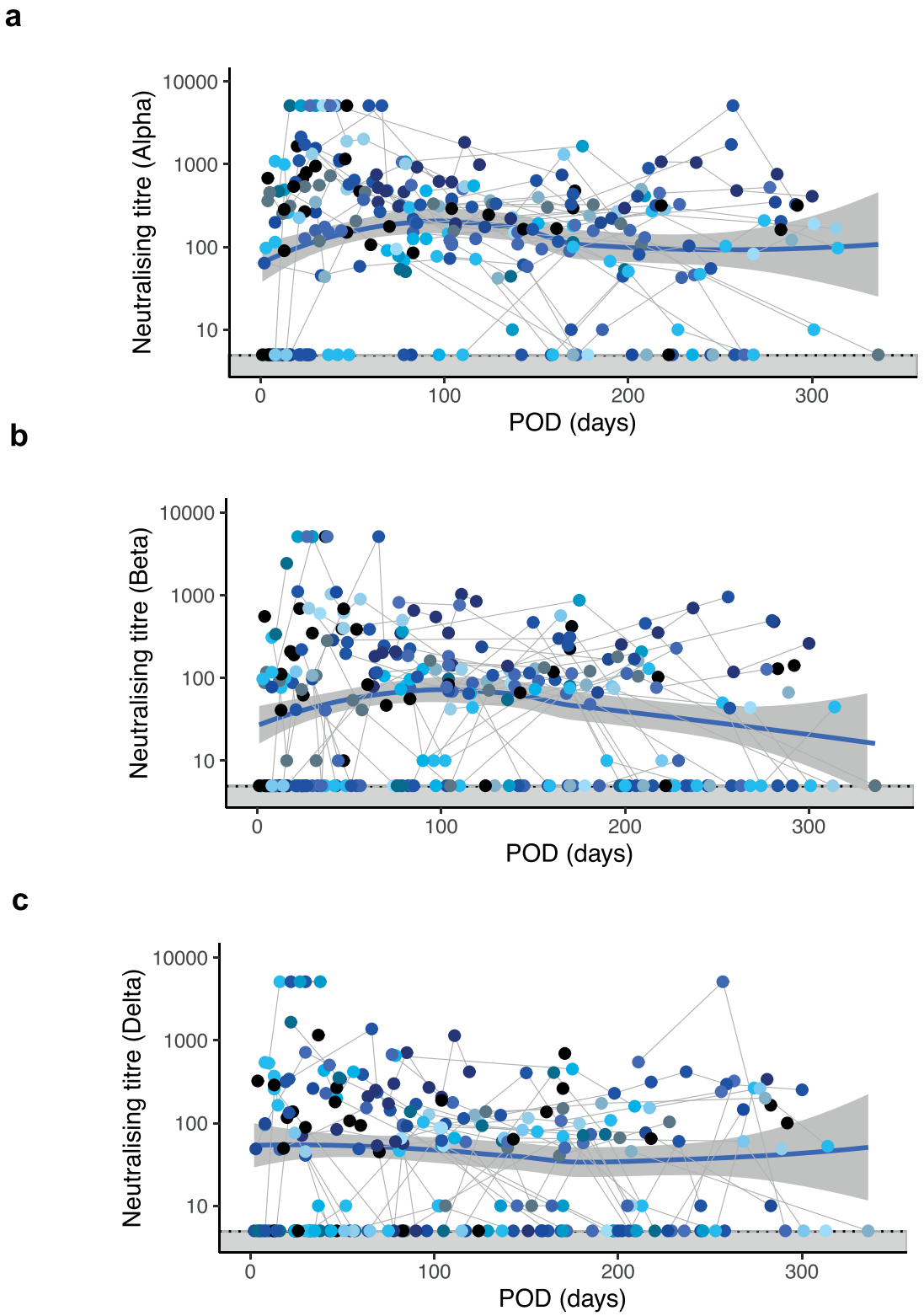

Extended Data Fig. 4 | Longitudinal assessment of NAb against VOCs. NAbT against **a)** Alpha, **b)** Beta, **c)** Delta over time POD. Black dots denote patients with only one sample, coloured dots denote patients with serial samples. Samples from individual patients are connected. Loess regression was performed and is displayed as a blue line with 95% confidence bands as grey area. Dotted lines and grey areas at graph bottom indicate limit of detection. POD, post onset of disease.

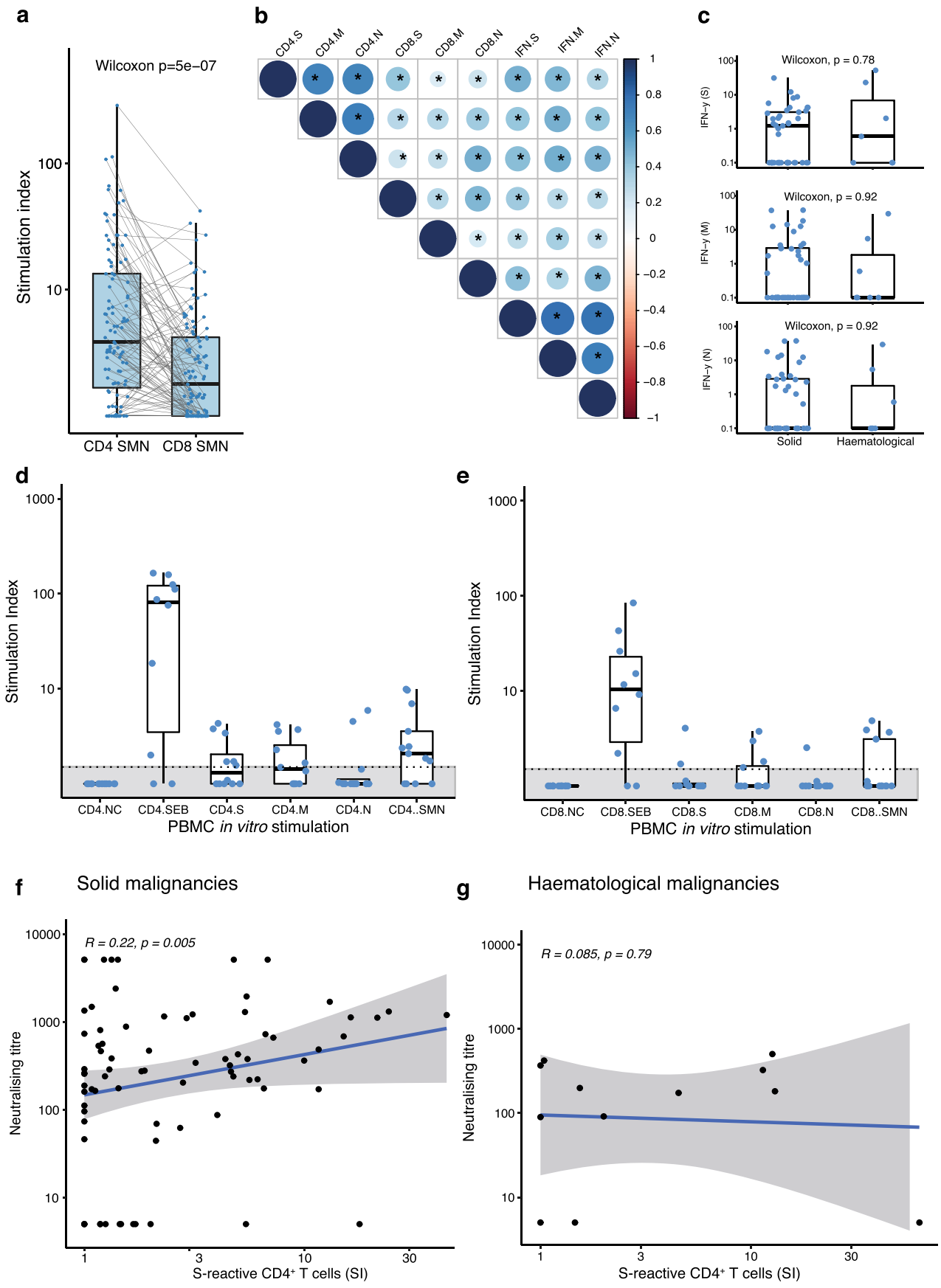

Extended Data Fig. 5 | See next page for caption.

Extended Data Fig. 5 | T-cell response in patients with cancer. a) Comparison between SARS-CoV-2 reactive $CD4^+$ and $CD8^+$ T cells evaluated in 100 patients with cancer. Boxes indicate the 25th and 75th percentiles, the median is shown, and whiskers indicate the 10th and 90th percentiles. Dots represent individual samples, connected dots are from the same sample. Significance as tested by two-sided Wilcoxon Mann Whitney U-test, p-values < 0.05 was considered significant. **b**) Pairwise spearman correlation of CD4 + and CD8 + T cells and IFN-γ concentration (pg/ml) in supernatants after stimulation of PBMCs (n = 82). Correlation is shown by color gradient. p-values for each correlation were calculated by two-sided t-test and were adjusted for multiple testing by Benjamini-Hochberg correction. P-value is denoted by size, in addition p-values < 0.05 are denoted by asterisk. *, $p < 0.05$. **c**) Comparison of IFN-γ concentration (pg/ml) in patients with solid (n = 41) and haematological malignancies (n = 8). Only patients in which SsT cells were detected were included. Significance as tested by two-sided Wilcoxon Mann Whitney U-test, p-values < 0.05 was considered significant. **d**) CD4 + T cells in 12 patients with cancer without confirmed SARS-CoV-2 infection. **e**) CD8 + T cells in 12 patients with cancer without confirmed SARS-CoV-2 infection. Boxes indicate the 25 and 75 percentiles, line indicates the median, and whiskers indicate the 10 and 90 percentiles. Dots represent individual samples. Correlation of S1-reactive AbT and SARS-CoV-2-specific CD4 + T cells in patients with **f**) solid (n = 81) and **g**) haematological malignancies (n = 19). Blue line denotes linear regression line with grey areas marking the 95% confidence band. Regression coefficient and p-values were computed by two-sided spearman regression, $p < 0.05$ was considered significant. NC, negative control, SEB, Staphylococcal enterotoxin B, IFN, IFN-γ.

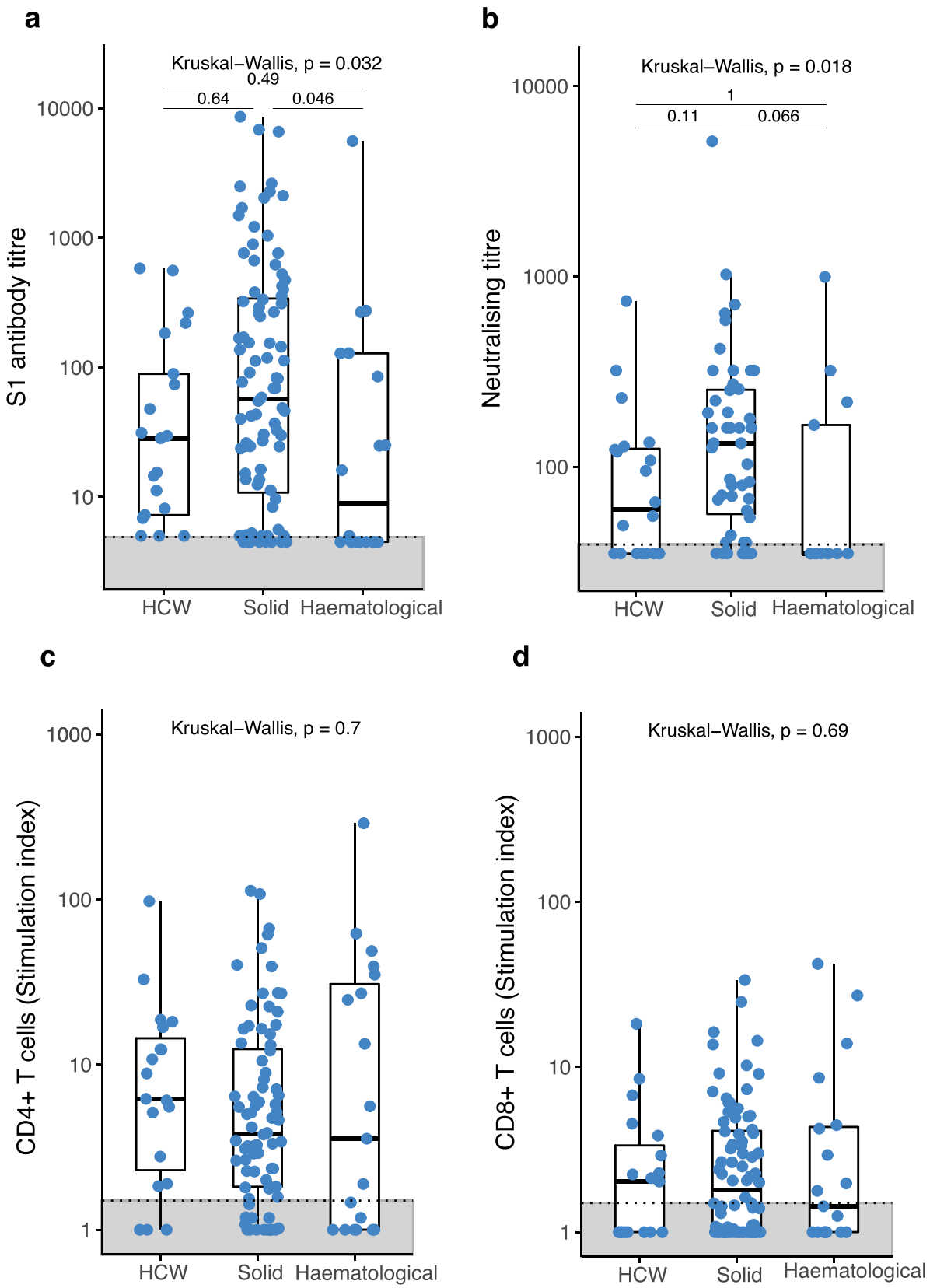

Extended Data Fig. 6 | Comparison of antibody and T-cell responses to individuals without cancer. Comparison of **a)** S1-reactive AbT and **b)** NAb against WT in HCW (n = 21), patients with solid malignancies (n = 92), and haematological malignancies (n = 20). Comparison of SARS-CoV-specific **c)** $CD4^+$ and **d)** $CD8^+$ T cells in HCW (n = 19), patients with solid malignancies (n = 81), and haematological malignancies (n = 19). Boxes indicate the 25 and 75 percentiles, line indicates the median, and whiskers indicate the 10 and 90 percentiles. Dots represent individual samples. Significance was tested by Kruskal Wallis test, $p < 0.05$ was considered significant, post-hoc test with Bonferroni correction was used for pairwise comparisons.

nature portfolio

Corresponding author(s): Samra Turajlic

Last updated by author(s): 16/09/2021

Reporting Summary

Nature Portfolio wishes to improve the reproducibility of the work that we publish. This form provides structure for consistency and transparency in reporting. For further information on Nature Portfolio policies, see our Editorial Policies and the Editorial Policy Checklist.

Statistics

For all statistical analyses, confirm that the following items are present in the figure legend, table legend, main text, or Methods section.

n/a	Confirmed
☐	☒ The exact sample size (*n*) for each experimental group/condition, given as a discrete number and unit of measurement
☐	☒ A statement on whether measurements were taken from distinct samples or whether the same sample was measured repeatedly
☐	☒ The statistical test(s) used AND whether they are one- or two-sided *Only common tests should be described solely by name; describe more complex techniques in the Methods section.*
☐	☒ A description of all covariates tested
☐	☒ A description of any assumptions or corrections, such as tests of normality and adjustment for multiple comparisons
☐	☒ A full description of the statistical parameters including central tendency (e.g. means) or other basic estimates (e.g. regression coefficient) AND variation (e.g. standard deviation) or associated estimates of uncertainty (e.g. confidence intervals)
☐	☒ For null hypothesis testing, the test statistic (e.g. *F*, *t*, *r*) with confidence intervals, effect sizes, degrees of freedom and *P* value noted *Give P values as exact values whenever suitable.*
☒	☐ For Bayesian analysis, information on the choice of priors and Markov chain Monte Carlo settings
☒	☐ For hierarchical and complex designs, identification of the appropriate level for tests and full reporting of outcomes
☒	☐ Estimates of effect sizes (e.g. Cohen's *d*, Pearson's *r*), indicating how they were calculated

Our web collection on statistics for biologists contains articles on many of the points above.

Software and code

Policy information about availability of computer code

Data collection	Data collection was conducted in Microsoft Excel for Mac Version 16.50
Data analysis	Data and statistical analysis were done in FlowJo 10.7.1 and R v3.6.1 in R studio v1.2.1335, Bio-Rad Everest software v2.4, Harmony 9, SciPy,

For manuscripts utilizing custom algorithms or software that are central to the research but not yet described in published literature, software must be made available to editors and reviewers. We strongly encourage code deposition in a community repository (e.g. GitHub). See the Nature Portfolio guidelines for submitting code & software for further information.

Data

Policy information about availability of data

All manuscripts must include a data availability statement. This statement should provide the following information, where applicable:

- Accession codes, unique identifiers, or web links for publicly available datasets
- A description of any restrictions on data availability
- For clinical datasets or third party data, please ensure that the statement adheres to our policy

All requests for raw and analysed data, and CAPTURE study protocol will be reviewed by the CAPTURE Trial Management Team, Skin and Renal Clinical Trials Unit, The Royal Marsden NHS Foundation Trust (CAPTURE@rmh.nhs.uk) to determine if the request is subject to confidentiality and data protection obligations. Materials used in this study will be made available upon request. There are restrictions to the availability based on limited quantities. Response to any request for data and/or materials will be given within a 28 day period. Data and materials that can be shared would then be released upon completion of a material transfer agreement.

Field-specific reporting

Please select the one below that is the best fit for your research. If you are not sure, read the appropriate sections before making your selection.

☒ Life sciences ☐ Behavioural & social sciences ☐ Ecological, evolutionary & environmental sciences

For a reference copy of the document with all sections, see nature.com/documents/nr-reporting-summary-flat.pdf

Life sciences study design

All studies must disclose on these points even when the disclosure is negative.

Sample size	The recruitment was conducted over approximately 9 months period at a national cancer centre thus representing a broad and realistic cancer patient population (adult patients). Recruitment to the infection cohort ceased once patients began receiving COVID-19 vaccination. The recruitment period was highly subject to changes given the dynamic situation of the pandemic and community infection rates and as the primary endpoint is descriptive so no power calculation was required. For each patient, all available samples were included in longitudinal analyses.
Data exclusions	No patients were excluded
Replication	For correlative measures, all human specimens underwent quality control (QC) assessments. Only those that passed QC were further analyzed. Inter-assay variation of the high-throughput neutralisation assay has been reported in Wall et al. Lancet 2021. Nanobodies were measured on each plate to normalise for replicative differences between variants and calibration is performed regularly. S1-reactive IgG was measured in duplicates, positive controls were run in quadruplicates to account for inter-assay variation. 1 Million viable cells were gated in flow assay. Positive and negative controls were included for each sample.
Randomization	There is no randomisation. This is an observational cohort study.
Blinding	Blinding was no performed. This is an observational cohort study.

Reporting for specific materials, systems and methods

We require information from authors about some types of materials, experimental systems and methods used in many studies. Here, indicate whether each material, system or method listed is relevant to your study. If you are not sure if a list item applies to your research, read the appropriate section before selecting a response.

Materials & experimental systems

n/a	Involved in the study
☐	☒ Antibodies
☐	☒ Eukaryotic cell lines
☒	☐ Palaeontology and archaeology
☒	☐ Animals and other organisms
☐	☒ Human research participants
☐	☒ Clinical data
☒	☐ Dual use research of concern

Methods

n/a	Involved in the study
☒	☐ ChIP-seq
☐	☒ Flow cytometry
☒	☐ MRI-based neuroimaging

Antibodies

Antibodies used	Antibody (Fluorochrom, Clone, Manufacturer, Catalogue No.): CD14 (V500, M5E2, BD, Catalogue No.: 561391), CD19 (V500, HIB19, BD, Catalogue No.: 561121),CD4 (BV605, OKT4, Biolegend, Catalogue No.: 317438), CD8 (BV650, RPA-T8, Biolegend: Catalogue No.: 301042), CD69 (PE-CF594, FN50, BD, Catalogue No.: 562617), OX40 (PE-Cy7, Ber-ACT35, Biolegend, Catalogue No.: 350012), CD137 (APC, 4B4-1, Biolegend, Catalogue No.: 309810), CD3 (AF700, OKT3, Biolegend, Catalogue No.: 317340) NSP8 (unconjugated, polyclonal, Antibodies online, Catalog No. ABIN233792) Goat Anti-Rabbit IgG (HRP Conjugate, polyclonal, Biorad, Cat No: 64371828), Alexa488-labelled-CR3009 antibody produced in-house. CR3022 anri-SARS-CoV-2 Ab (unconjugated, CR3022, Absolute Antibodies, Catalogue No.: Ab01680-10.0)
Validation	Antibodies for AIM assay were chosen on the basis of previous publication of the assay (Grifoni et al. Targets of T Cell Responses to SARS-CoV-2 Coronavirus in Humans with COVID-19 Disease and Unexposed Individuals. Cell, 2020) References with validation of other primary antibodies used are as follows: Neutralising antibodies (NSP8 and anti-rabbit IgG - Wrobel et al. Antibody mediated disruption of the SARS-CoV-2 spike glycoprotein. Nat Comm, 2020), Alexa488-labelled-CR3009 antibody (Wall et al. Neutralising antibody activity against SARS-CoV-2 VOCs B.1.617.2 and B.1.351 by BNT162b2 vaccination, Lancet, 2021). CR3022 (Ng. et al. Preexisting and de novo humoral immunity to SARS-CoV-2 in humans. Science, 2020).

Eukaryotic cell lines

Policy information about cell lines

Cell line source(s)	VERO-E6 cells were from the National Institute for Biological Standards and Control, UK. The SARS-CoV-2 isolate hCoV-19/England/02/2020 was obtained from the Respiratory Virus Unit, Public Health England, UK, and propagated in Vero E6 cells.
Authentication	We authenticated the VERO-E6 cells using a species ID Molecular test using AGM specific primers and the cell line gives a match with our controls for African Green monkey. We further tested the cell line with Human STR Authentication to prove that there was no evidence of cross contamination with human lines and Veros gave a distinct pattern of peaks on Human STR.
Mycoplasma contamination	Lines were screened for mycoplasma contamination.
Commonly misidentified lines (See ICLAC register)	N/A

Human research participants

Policy information about studies involving human research participants

Population characteristics	Adult patients with current or history of invasive cancer were eligible for enrolment. Inclusion criteria for CAPTURE are intentionally broad, and patients are recruited irrespective of cancer type, stage, or treatment. 357 unvaccinated cancer patients were evaluable and followed-up for a median of 154 days (IQR: 63 - 273). Median age was 60 years, 54% were male, 89% had solid malignancy, and the majority (64%) had advanced disease (Table 1). Overall, 118 patients (33%) were SARS-CoV-2-positive confirmed by positive SARS-CoV-2 RT-PCR or ELISA for S1-reactive antibodies (laboratory case definition), including 97 patients with solid cancers and 21 with haematological malignancies (Figure 1A). The most common comorbidities were hypertension (27%), obesity (21%) and diabetes mellitus (11%), and no significant differences were observed in baseline demographics between patients with solid and haematological malignancies.
Recruitment	CAPTURE study (NCT03226886) inclusion criteria are intentionally broad, and patients were approached irrespective of cancer type, stage, or treatment. CAPTURE included targeted recruitment arms to include both patients with clinically suspected/confirmed SARS-CoV-2 infection (Group A; key point of recruitment was a dedicated clinical assessment unit for patients with symptoms suggestive of COVID-19 irrespective of severity) and patients with no symptoms suggestive of SARS-CoV-2 infection in the course of their cancer care (Group B; key point of recruitment were outpatient clinics). Distinct from a population screening program, this approach led to a higher proportion of SARS-CoV-2 infected patients (around 30% of patients recruited) relative to expected population prevalence, but nevertheless representative of the broad range of COVID-19 presentations due to the recruitment of all-comers in Arm B.
Ethics oversight	CAPTURE was approved as a substudy of TRACERx Renal (NCT03226886). TRACERx Renal was initially approved by the NRES Committee London - Fulham on January 17, 2012. The TRACERx Renal sub-study CAPTURE was submitted as part of Substantial Amendment 9 and approved by the Health Research Authority on April 30, 2020 and the NRES Committee London - Fulham on May 1, 2020. CAPTURE is conducted in accordance with the ethical principles of the Declaration of Helsinki, Good Clinical Practice and applicable regulatory requirements. All participants required written informed consent to participate.

Note that full information on the approval of the study protocol must also be provided in the manuscript.

Clinical data

Policy information about clinical studies

All manuscripts should comply with the ICMJE guidelines for publication of clinical research and a completed CONSORT checklist must be included with all submissions.

Clinical trial registration	CAPTURE study (NCT03226886)
Study protocol	Request for protocols should be directed to CAPTURE trials unit via CAPTURE@rmh.nhs.uk
Data collection	Data from between May 4, 2020 and March 31st 2021 (database lock) was collected at Royal Marsden hospital hospital, by extract from clinical records approved as per protocol.
Outcomes	Primary endpoint of study is description of population characteristics between SARS-CoV-2 positive and negative cancer patients - as this is a planned interim analysis the primary endpoint has not yet been assessed. Secondary endpoints and exploratory endpoints are differences in overall survival, intensive treatment unit admission rate, anti-cancer treatment received, and characterising clinical and immunological determinants of COVID-19 severity in cancer patients. This planned interim analysis pertains to characterising clinical and immunological determinants of COVID-19 severity in cancer patients; humoural and cellular components of the immune response are quantified and then associations with patient, cancer and treatment specific factors are assessed in a multivariate model (see methods).

Flow Cytometry

Plots

Confirm that:

☒ The axis labels state the marker and fluorochrome used (e.g. CD4-FITC).

☒ The axis scales are clearly visible. Include numbers along axes only for bottom left plot of group (a 'group' is an analysis of identical markers).

☒ All plots are contour plots with outliers or pseudocolor plots.

☒ A numerical value for number of cells or percentage (with statistics) is provided.

Methodology

Sample preparation	Whole blood was collected in EDTA tubes (VWR) and stored at 4ºC until processing. All samples were processed within 24 hours. Time of blood draw, processing, and freezing was recorded for each sample. Prior to processing tubes were brought to room temperature (RT). PBMC and plasma were isolated by density-gradient centrifugation using pre-filled centrifugation tubes (pluriSelect). Up to 30 ml of undiluted blood was added on top of the sponge and centrifuged for 30 minutes at 1000 x g at RT. Plasma was carefully removed then centrifuged for 10 minutes at 4000 x g to remove debris, aliquoted and stored in liquid nitrogen. The cell layer was then collected and washed twice in PBS by centrifugation for 10 minutes at 300 x g at RT. PBMC were resuspended in Recovery cell culture freezing medium (Fisher Scientific) containing 10% DMSO.
Instrument	All experiments were run on a Bio-Rad Ze5 flow cytometer running Bio-Rad Everest software v2.4
Software	Data were analysed using FlowJo 10.7.1
Cell population abundance	Cells were not sorted in this study
Gating strategy	Lymphocytes were gated in FSC-A/SSC-A plot, followed by gating for singlets by plotting FSC-A vs. FSC-H. Viable CD3+ cells were identified by plotting CD3 vs. CD14,CD19, and viability dye. Next CD4+ and CD4+ cells were gated and finally CD137 +OX40+ cells were identified in the CD4+ population and CD137+CD69+ in the CD8+ population.

☒ Tick this box to confirm that a figure exemplifying the gating strategy is provided in the Supplementary Information.